

A  
Dissertation  
On

# Synthesis and Characterization of Single Walled Carbon Nanotubes

Submitted in partial fulfillment of the requirement  
For the award of the degree of

**MASTER OF TECHNOLOGY**

In  
**(Nano Science and Technology)**



Submitted by

**Sugandh Kumar**

**Roll No. 2K10/NST/14**

Under the Guidance of

**Dr. Pawan Kumar Tyagi**

**Assistant Professor**

**DEPARTMENT OF APPLIED PHYSICS  
DELHI TECHNOLOGICAL UNIVERSITY  
BAWANA ROAD, DELHI- 110042  
July 2012**

## **ACKNOWLEDGEMENT**

Now the final report is in my hands. It is not a one night venture; it requires firm determination, dedication, warmth bliss and grace of the Formless one that equips me to perform this task. A formal statement of acknowledgement will hardly meet the end of justice while writing these words, I feel obliged to all of them who extended their inconceivable co-operation towards the achievement of whatever we have achieved.

First of all I would like to express deep sense of gratitude and sincere thanks to my supervisor **Dr. Pawan Kumar Tyagi, Assistant Professor, Delhi Technological University, New Delhi** for providing experimental arrangements at Nanofabrication lab, DTU and making available literature and other facility. Constant supervision of my guide throughout the project, learned guidance and invaluable suggestions helped me to complete the project well in stipulated time. A deep sense of gratitude is expressed to **Dr. Brajesh S. Yadav, Scientist E-II Characterization of Materials Lab, Solid State Physics Laboratory, DRDO, New Delhi** for his contribution to this work.

With due regards, I express sincere thanks to **Dr. R. K. Sinha, Head of Applied Physics Department, DELHI TECHNOLOGICAL UNIVERSITY, NEW DELHI**, for his valuable suggestions and support.

I am deeply overwhelmed to my Lab mates namely **Mr. Randeep Kundu & Mr. Parichay Jindal** for their help and kind attitude. Their appreciation and encouragement in all respect are really unforgettable for me.

Also I express deep sense of gratitude and sincere thanks to **Dr. R. Bhattacharya** and all the faculty members **Dr. A.K Jha, Dr. Mohan S.Mehata, Dr. Rishu Chaujur, Dr. Yogita Kalra, Dr. Ajeet Kumar, Dr. Nitin K. Puri, Dr. M. Jayasimhadri, Dr. Amrish K. Panwar** who has been part of my M.Tech program at Delhi Technological University during course work and has helped me in my research.

Finally I would like to thank my parents and other family members who were always anxious to help me & contributed a major driving force behind the completion of this project.

**Sugandh Kumar**

**M.Tech (NST) - 14/NST/2k10**

**Delhi Technological University**

**Date:**

**Place:**

## **Certificate**

This is to certify that **Mr. Sugandh Kumar** has done a research Work on the topic entitled “**Synthesis and Characterization of Single Walled Carbon Nanotubes**” under my supervision. The present research work is being submitted to **Department of Applied Physics, Delhi Technological University (Formerly Delhi College of Engineering)**, in partial fulfillment of the requirement for the award of the degree of Master of Technology in Nanoscience and Technology, embodies faithful record of research work carried out by Mr. Sugandh Kumar. He has worked under my guidance and that this work has not been submitted, in part or full, for any other degree of Delhi Technological University or any other university.

**Dr. Pawan Kumar Tyagi**  
**Assistant Professor**  
**Department of Applied Physics**  
**Delhi Technological University**

**Date:**

**Place:**

## **Abstract**

The revolutionary discovery of carbon nanotubes (CNTs) in 1991 by Sumio Iijima further led to powerful research in the field of science. The attractive properties of this unique materials has opened a great number of potential applications e.g. one dimensional conductors, super capacitors, reinforcing fibers, hydrogen storage, electron field emitters & also in the field of medical sciences. Even with rapid technical progresses there is still much great effort required in the development of a synthesis method suitable for commercial applications. A foremost runner is the chemical vapour deposition (CVD) technique.

Nucleation and growth of CNTs are induced by the decomposition of carbon-containing gases such as - CO, CO<sub>2</sub>, CH<sub>4</sub>, C<sub>2</sub>H<sub>4</sub> etc, over a metallic catalyst at temperatures between 600 °C and 1400 °C. CVD is the most widely used technique to produce CNTs in large quantities and much development has been done in its synthesis from the point of view of cost reduction, mass production & purification techniques. But the greatest challenge of CVD process remains with the growth mechanism. In CNT Synthesis by CVD method is the most important reaction step seems to be diffusion of carbon through the metal catalyst and the most active metals like iron, cobalt and nickel. But their catalytic action depends upon the type of precursor, the type of substrate and the reactive gases used. Till date few investigations of the chemical and morphological evolution of the catalyst during CVD process have been performed.

This thesis mainly focuses on the synthesis and characterization of single walled carbon nanotube using Iron/Cobalt - Molybdenum - Magnesium oxide (Fe/Co: Mo: MgO) based catalysts under the gases like Argon and Methane atmosphere between 27 °C and 875 °C. The main reaction took place at 875 °C for 20 minutes which results in the growth of CNT.

According to the nature of the catalyst during synthesis we optimize atmosphere of gases, their flow rate and temperature at which reaction has to be carried out. After the reaction, samples were cooled down by microprocessor based controller from 875 °C to 27 °C in the argon atmosphere. The microscopic images showed that iron, molybdenum and magnesium can be used for typical nanotube synthesis as catalyst for CNT nucleation and growth.

Grain size reduction during reactions in the catalyst precursor and the transformation of precursors into metallic phase are the main requirements for nanotube growth. The reaction during the reduction of the precursor is further related with the nucleation and growth of nanotubes. In case of iron based catalyst system, where the breakdown of metastable carbides act as a boost of nanotube formation, the emergence of carbides in the molybdenum system after 20 minutes stops further carbon nanotube growth.

# Table of Contents

Acknowledgement	II
Certificate	IV
Abstract	V
List of Figures	IX
List of Tables	XI
<b>Chapter1: Introduction &amp; History of CNT</b>	<b>1</b>
1.1 Introduction & History of Carbon Nanotubes	1
1.2 Carbon Allotropes	3
1.3 Carbon Nanotubes	4
1.4 Classification of CNT	5
1.4.1 Armchair, Zigzag & Chiral CNT	6
1.5 Properties of CNT	8
1.6 Synthesis Methods	10
1.6.1 Arc Discharge Method	10
1.6.2 Laser Ablation Method	11
1.6.3 Chemical Vapour Deposition	12
1.6.4 Ball Milling	13
1.6.5 Other Methods	13
1.7 Applications of CNT	14
1.7.1 Field Emission	14
1.7.2 Conductive Plastics	15
1.7.3 Energy Storage	15
1.7.4 Conductive Adhesives and Connectors	16
1.7.5 Molecular Electronics	16
1.7.6 Thermal Materials	16
1.7.7 Structural Composites	17
1.7.8 Fibers and Fabrics	17

1.7.9	Catalyst Supports	17
1.7.10	Biomedical Applications	17
1.7.11	Other Applications	18
<b>Chapter 2: Literature Review</b>		<b>19</b>
<b>Chapter 3: Experimental Setup and Techniques</b>		<b>27</b>
3.1	Introduction of Techniques	27
3.2	Chemical Vapour Deposition (CVD) System	29
3.2.1	Types of CVD	30
3.2.2	Basic Diagram of CVD & Lab Setup	30
3.2.3	Carbon Precursor	33
3.2.4	Temperature	34
3.2.5	Catalyst Nanoparticle	34
3.2.6	Gas Flow Rates	35
3.3	Field Emission Scanning Electron Microscopy (FESEM)	37
3.4	Transverse Electron Microscope (TEM)	39
<b>Chapter 4: Experimental Methodology</b>		<b>47</b>
4.1	Accessories Required	47
4.2	Experimental Condition & Procedure	47
<b>Chapter 5: Results and Discussion</b>		<b>49</b>
5.1	FESEM Images of CNTs	49
5.2	TEM Images of CNTs	54
<b>Chapter 6: Conclusion</b>		<b>58</b>
<b>References</b>		<b>60</b>



## List of Figures

- 1) Figure 1.1 Schematic diagram of (a) Graphene (b) Bent Graphene (c) Carbon Nanotube
- 2) Figure 1.2 Schematic diagrams of different allotropes of Carbon
- 3) Figure 1.3 Schematic diagrams of (a) Single Walled CNT (b) Double Walled CNT (c) Multi Walled CNT
- 4) Figure 1.4 Finite Graphene sheet that define roll up or unit vectors
- 5) Figure 1.5 Sheet of Graphene Sheet Rolled into different CNTs
- 6) Figure 1.6 Showing Different type of CNT based on Chiral Angles
- 7) Figure 3.1 Current CNT growth mechanism hypotheses
- 8) Figure 3.2 Schematic diagram of Chemical Vapour Deposition Setup
- 9) Figure 3.3 Microprocessor based Controller
- 10) Figure 3.4 Different gas flow controllers and mixtures
- 11) Figure 3.5 Side View of Microprocessor Controlled Furnace
- 12) Figure 3.6 Different Cylinders containing 3 gases as argon, methane & hydrogen
- 13) Figure 3.7 Water filled beaker in which Argon is fed through to avoid the oxidation
- 14) Figure 3.8 General growth modes of CNT in CVD
- 15) Figure 3.9 Basic Model of Field Emission Scanning Electron Microscope
- 16) Figure 3.10 Internal Diagram of Field Emission Scanning Electron Microscope.
- 17) Figure 3.11 Basic Internal Transverse Electron Microscope
- 18) Figure 3.12 Diagram showing the difference in internal structure of LM, TEM, SEM
- 19) Figure 3.13 Basic diagram of Charge distribution in TEM
- 20) Figure 3.14 Electromagnetic Converging lens of Electron Microscope
- 21) Figure 3.15 Show actual path of electron in TEM

- 22) Figure 3.16 Show different Parts of Transverse Electron Microscope
- 23) Figure 4.1 Experimental Condition Chart
- 24) Figure 5.1: SEM images of the SWCNTs grown in thermal CVD using (Fe: Mo: MgO) catalyst at same magnifications (scale bar at 10 nm)
- 25) Figure 5.2: SEM images of the SWCNTs grown in thermal CVD using (Fe: Mo: MgO) catalyst at various magnifications (scale bar of two image at 10 nm & other two at 100 nm)
- 26) Figure 5.3: SEM images of the SWCNTs grown in thermal CVD using (Fe: Mo: MgO) catalyst at same magnifications (scale bar at 100 nm)
- 27) Figure 5.4: SEM images of the SWCNTs grown in thermal CVD using (Co: Mo: MgO) catalyst at various magnifications (scale bar at 100 nm) \*
- 28) Figure 5.5 Bright field TEM images of the carbon nanotube grown in thermal CVD using ferrocene used as catalyst (scale bars are 2000 nm & 1000 nm) \*
- 29) Figure 5.6 The TEM images of as grown metal-filled MWCNT \*

The “\*” mark in this dissertation indicate that data has been shared with Mr. Parichay Jindal as we belong to the same group.

## **List of Tables**

- 1) Table 2.1 Synthesis of CNTs by Using Different Techniques
- 2) Table 2.2 Synthesis of CNTs by Using Different Carbon Precursors

# Chapter 1

## Introduction

### 1.1 Introduction & History of Carbon Nanotubes <sup>[1]</sup>

We know that carbon is chemical element having atomic number 6 and a member of group 14 in the periodic table. It is one of the most abundant elements found in the nature. It is having six electrons which occupy  $1s^2$ ,  $2s^2$  and  $2p^2$  atomic orbital. It has ability to hybridize in  $sp$  (e.g.  $C_2H_2$ ),  $sp^2$  (e.g. graphite) and  $sp^3$  (e.g.  $CH_4$ ) forms <sup>[2]</sup>. Many allotropes of carbon  $sp^2$  hybridized have been discovered which are of nano dimensions such as fullerenes, carbon nanotubes, amorphous carbon, graphene etc <sup>[3]</sup>. They have enthused to the research activity at world level. Theoretically, graphene was considered as evident material of the carbon nanotubes. It is therefore useful to understand this material first.

In 1970's, Morinobu Endo <sup>[4]</sup> prepared the first carbon filament of nanometer dimensions. Till 1980, we were only familiar with the three forms of carbon: diamond, graphite and amorphous carbon. The first hollow cage of carbon like Buckminsterfullerene also known as the Buckyball or  $C_{60}$  fullerene was discovered by Richard E. Smalley in 1985 <sup>[5]</sup>. Out of more than forty forms of fullerenes,  $C_{60}$  is the first spherical carbon molecule, with carbon atoms arranged in a soccer ball shape. The other most common structure is known as  $C_{70}$ . It is slightly elongated & spherical carbon molecule which resembles like a rugby ball. In 1991, first invention of nanotube (multi walled carbon nanotube) was done by Sumio Iijima at IBM with the use of arc-evaporation technique. Further in 1993 that, Sumio Iijima and Donald Bethune found single walled nanotubes known as CNTs (Bucky tubes) <sup>[6]</sup>.

CNT can be visualized as cylindrical rolled of single layer i.e. one-atomic thick sheet of graphite. The electronic and mechanical properties of carbon nanotubes strongly depend on the rolling angle and curvature (i.e. depends on the width of graphene).

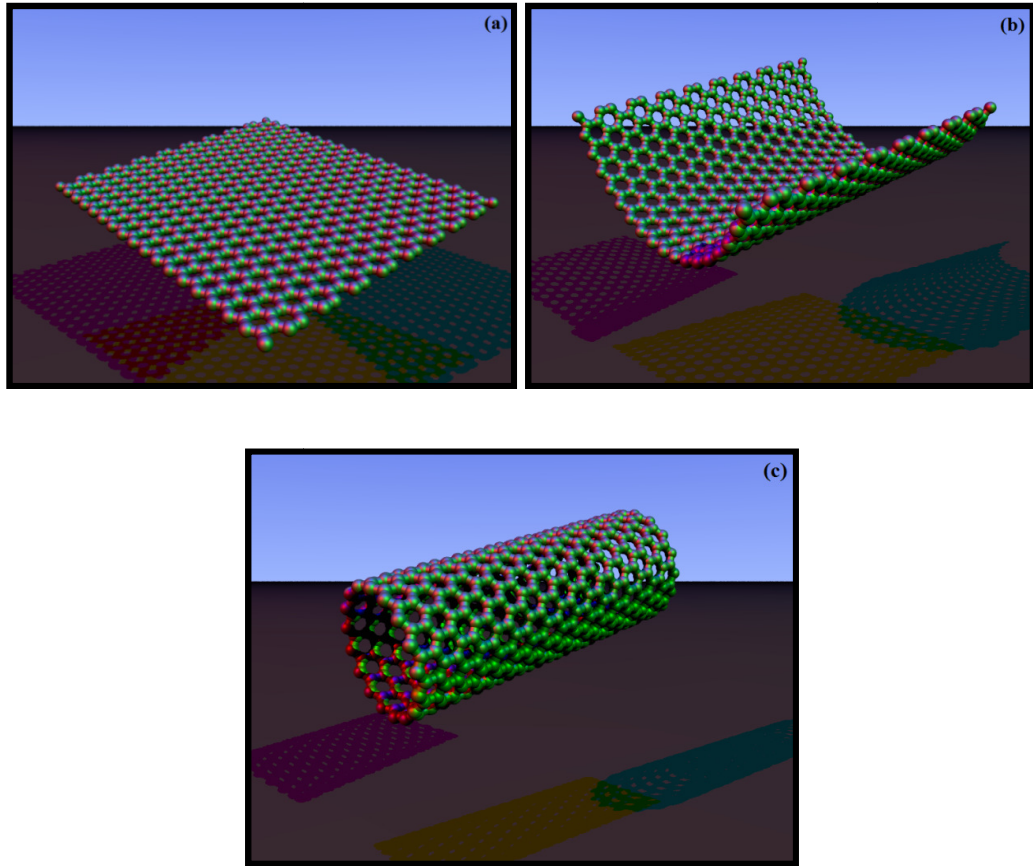


**Figure 1.1** Schematic diagram of (a) Graphene (b) Bent Graphene (c) Carbon Nanotube <sup>[6]</sup>

## 1.2 Carbon Allotropes

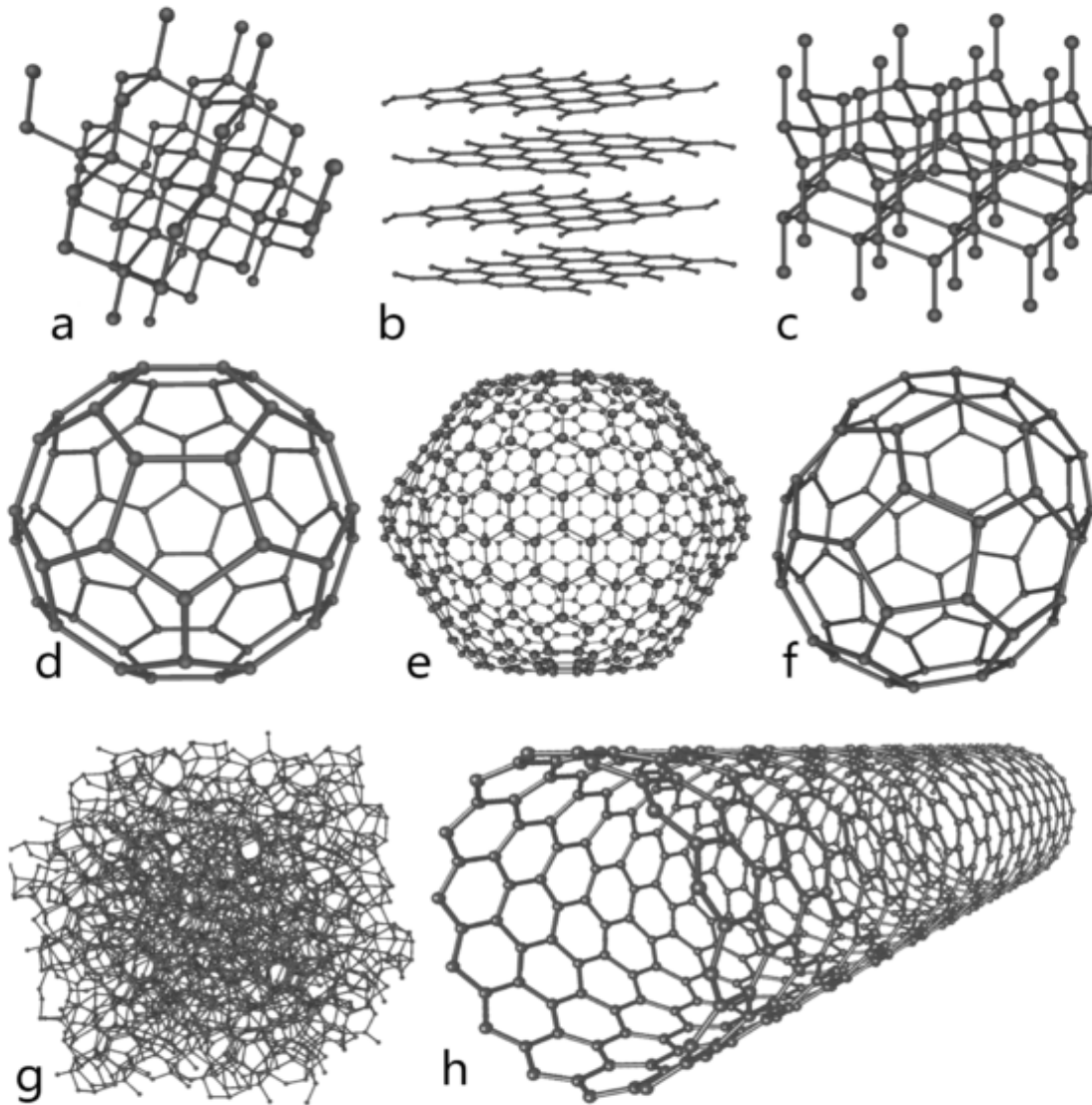


**Figure 1.2** Schematic diagrams of different allotropes of carbon <sup>[7]</sup>

a) Diamond

b) Graphite

c) Lonsdaleite

d) C<sub>60</sub> (Buckminsterfullerene)

e) C<sub>540</sub> (Fullerene)

f) C<sub>70</sub> (Fullerene)

g) Amorphous carbon

h) Single Walled Carbon Nanotubes

## 1.3 Carbon Nanotubes

CNT is a type of carbon allotrope that consists of carbon elements integrated in a tube shaped like those of a hexagonal honeycomb structure<sup>[8]</sup>. A Carbon Nanotube is a tube-shaped carbon material, having a diameter measuring on the nanometer scale. With the diameter in nanometers ( $1\text{nm} = 10^{-9}\text{ m}$ ), CNT is a substance of an extremely small domain. A nanometer is about one ten thousandth of the thickness of a human hair. The graphite layer appears somewhat like a rolled-up chicken wire with a continuous unbroken hexagonal mesh and carbon molecules at the apexes of the hexagons.

Carbon Nanotubes typically have diameters ranging from 1 nm up to 50 nm. The length typically varies till several microns, but recent advancements have made the nanotubes much longer and they have found to be in centimeters. Nanotubes are composed of  $sp^2$  bonds, which are similar to those observed in graphite and they naturally align themselves into ropes held together by Vander-Waals forces.

Simply, carbon nanotubes exist as a macro-molecule of carbon, analogous to a sheet of graphite (the pure, brittle form of carbon in your pencil lead) rolled into a cylinder while graphite looks like a sheet of chicken wire, a tessellation (process of creating a two-dimensional plane using the repetition of a geometric shape with no overlaps and no gaps) of hexagonal rings of carbon<sup>[8]</sup>. Sheets of graphite in the pencil stacked on top on one another but they can slide on each other and can be separated easily, that is why they can be used for writing. However, when coiled the carbon arrangement becomes very strong. Indeed, nanotubes have been known to be up to one hundred times as strong as steel and almost two millimeters long. These nanotubes have a hemispherical cap at each end of the cylinder. They are light, flexible, thermally stable, and chemically inert. They have the ability to be either metallic or semi-conducting depending on the twist of the tube.

## 1.4 Classification of CNT

Basically CNT is divided into 3 types on the basis of their Structure. They are

- a) Single Walled CNT
- b) Double Walled CNT
- c) Multi Walled CNT

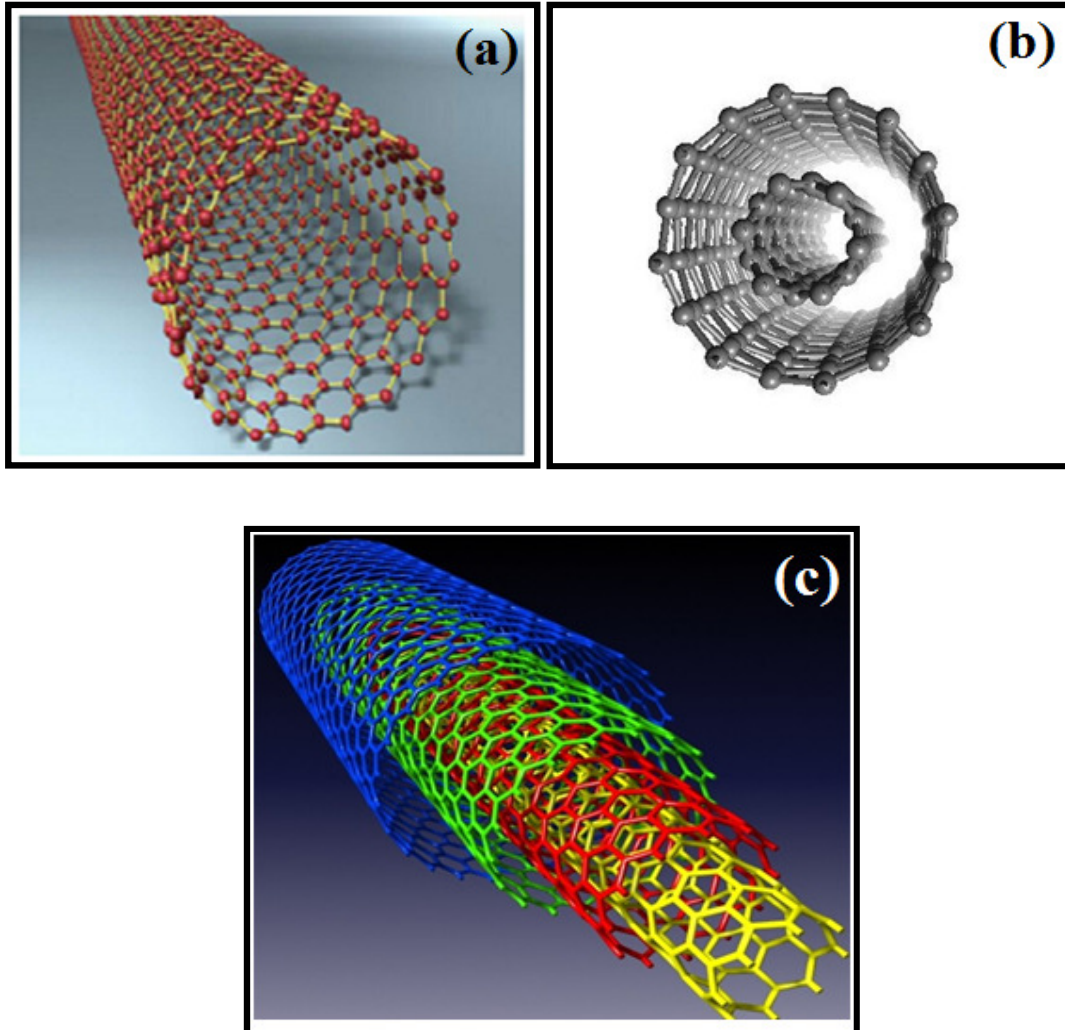


**Figure 1.3** Schematic diagrams of (a) Single walled CNT (b) Double walled CNT (c) Multi walled CNT <sup>[9]</sup>



### 1.4.1 Armchair, Zigzag and Chiral CNT

Depending upon the way the graphene sheet is wrapped gives another classification of CNTs. The wrapping is represented by a pair of indices (n, m). The integer n and m denote the number of unit vectors along two directions in the honeycomb crystal lattice of graphene. If m = 0, the nanotubes are called zigzag nanotubes, and if (n=m), the nanotubes are called armchair nanotubes. Otherwise, they are called Chiral. The diameter (d) of an ideal nanotube can be calculated from its (n, m) indices as follows <sup>[10]</sup>:

$$d = \frac{a}{\pi} \sqrt{(n^2 + nm + m^2)}.$$

Where, a = 0.246 nm

n, m = number of unit vectors

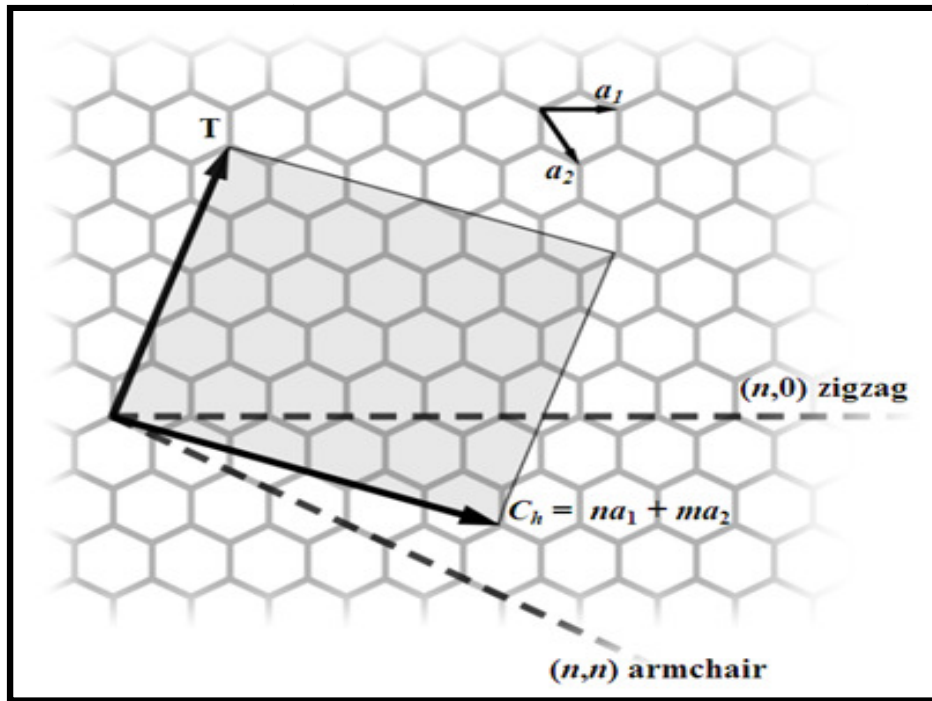


**Figure 1.4** Finite graphene sheet that define roll up or unit vectors <sup>[10]</sup>

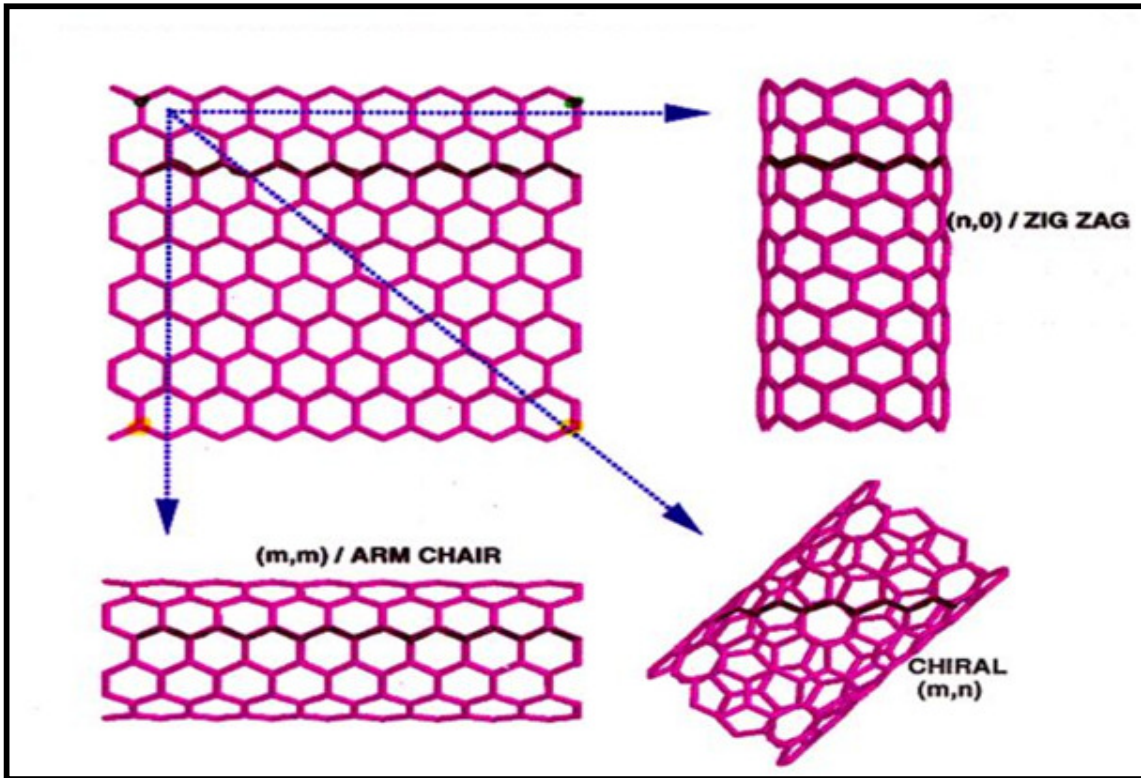


Figure 1.5 Sheet of graphene rolled into different CNTs [11]

Now depending upon chiral angles CNTs can be further classified as:

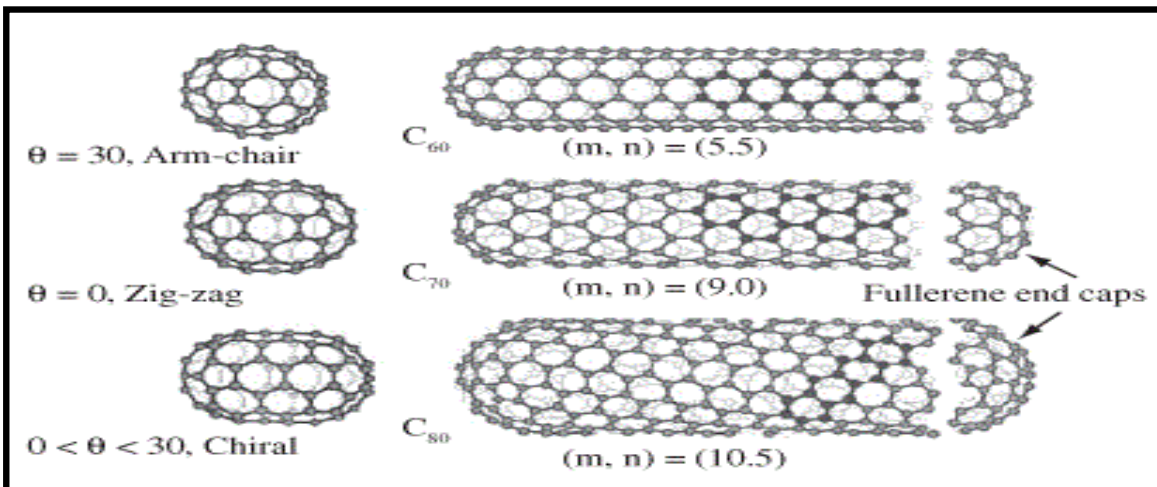


Figure 1.6 Showing different type of CNT based on chiral angles [12]

## 1.5 Properties of CNT <sup>[13]</sup>

(a) **Size:** It is a quasi 1D solid. Nanostructures with dimensions of ~1 nm diameter (~10 atoms around the cylinder). The length is around few micrometers ( $\mu\text{m}$ ).

High aspect ratio: 
$$\frac{\text{length}}{\text{diameter}} > 1000$$

(b) **Electronic Properties:** Can be either metallic or semiconducting depending on diameter and orientation of the hexagons.

$$C_h = n \vec{a}_1 + m \vec{a}_2 \quad \text{If, } \frac{2n+m}{3} = i \quad \begin{array}{l} \text{then metallic} \\ \text{Else, semiconducting} \end{array}$$

In simple words we can say that if  $(n = m)$  then tube is metallic & if  $(n - m)$  is divisible by 3 then it is semiconducting.

- Current capacity

Carbon nanotube: 1 GAmps /  $\text{cm}^2$

Copper wire: 1 MAmps /  $\text{cm}^2$

(c) **Mechanical Properties:** Very high strength, modulus, and resiliency. Good properties on both compression and extension. It is Strong like steel, light like Aluminum & elastic like a plastic.

- Heat transmission

Comparable to pure diamond (3320 W / m·K)

- Temperature stability

Carbon nanotube: 750 °C (in air)

Metal wires in microchips: 600 - 1000 °C

(d) **Thermal Properties:** All nanotubes are expected to be very good thermal conductors along the tube, exhibiting a property known as ballistic conduction but good insulators laterally to the tube axis.

(e) **Optical Properties:** The optical properties include absorption, photoluminescence and raman spectroscopy of carbon materials. By changing the different parameters presented during synthesis of nanotube, affect the size and quality of nanotube. So, these characterization techniques characterize the quality of CNTs and defects produced.

## 1.6 Synthesis Methods <sup>[14]</sup>

There are many methods of making CNTs. First of all, fullerenes were observed after vaporizing graphite with a short-pulse, high-power laser. However the method was not the perfect method for commercial purpose. CNTs have probably been around for a lot longer period but due to unavailability of electron microscopy at that time they were not invented. The first method for producing CNTs and fullerenes in reasonable quantities was by arc current method in which we apply an electric current across two carbonaceous electrodes in an inert gas atmosphere & the method is called plasma arcing. It involves the evaporation of one electrode as cations followed by deposition at the other electrode. Fullerenes and CNTs are formed by plasma arcing of carbonaceous materials specially graphite. The fullerenes appear in the soot that is formed when CNTs are deposited on the opposing electrode. Another method of nanotube synthesis is the plasma arcing in the presence of cobalt, iron with slight concentration. However when iron is added as a catalyst, the nature of the product changes to a web with thickness that stretches from the cathode to the walls of the reaction vessel. The mechanism by which iron changes this process is ambiguous, still one possibility is that such metals affect the local electric fields and thus the formation of the five-membered rings can be obtained. At present time, CVD is the most convenient & cheapest way for the synthesis of Carbon related materials like CNTs, Graphene for research & commercial purposes.

### 1.6.1 Arc Discharge

The carbon arc discharge method which was initially used for producing C<sub>60</sub> fullerenes is now the most common simplest & easiest way to produce CNTs. However, it is a technique which produces a complex mixture of components and requires further purification to separate the CNTs from complex mixture. This method creates CNTs through arc-vaporization using two carbon rods placed end to end which are separated by approximately 1mm in an enclosure

that is usually filled with inert gas at low pressure. Modern techniques have shown that it is also possible to create CNTs with the arc method in liquid nitrogen. The discharge vaporizes the surface of one of the carbon electrodes and forms a small rod-shaped deposit on the other electrode. Depending on the uniformity of the plasma arc and temperature of the deposition on the carbon electrode produces CNTs in large quantity.

### **1.6.2 Laser Ablation**

In 1996 CNTs were first synthesized by using a dual-pulsed laser and achieved large amount than 70 wt % purity. Samples were prepared by laser vaporization of graphite rods with a 50:50 catalyst mixture of cobalt, iron and nickel at 1200 °C in the atmosphere of argon, followed by heat treatment in a vacuum at 1000 °C to remove the C<sub>60</sub> and other fullerenes. The initial laser vaporization pulse was followed by a second pulse in order to vaporize the target more uniformly. The use of two successive laser pulses minimizes the amount of carbon deposited as filth. The second laser pulse breaks up the larger particles ablated by the first and feeds them while growing nanotube structure. Each rope is found to consist primarily of a bundle of single walled nanotubes aligned together along a common axis. By varying the growth temperature, catalyst composition and other process parameters the average nanotube diameter and size distribution can be varied. Arc-discharge and laser vaporization are currently the principal methods for obtaining small quantities of high quality CNTs. However, both methods have to suffer from drawbacks. They involve evaporating the carbon source, so it has been unclear how to scale up production to the industrial level by using these approaches. The second issue deals with the fact that vaporization methods grow CNTs in highly tangled forms, mixed with unwanted forms of carbon and metal species. The CNTs produced are difficult to purify, manipulate, and assemble for building nanotube device for practical purposes.

### 1.6.3 Chemical Vapour Deposition

For the last twenty five years chemical vapor deposition has been used to produce the Carbon Nanotubes & other carbon materials. It is generally used for hydrocarbons over a metal catalyst that has carbon materials as carbon fibers and filaments. Large amounts of CNTs can be produced by catalytic CVD of acetylene over cobalt and iron catalysts supported on silica. The carbon deposition activity seems to relate the cobalt/iron content of the catalyst whereas the CNT's seems to be selectivity a function of the pH in catalyst preparation. Fullerenes as well as bundles of single walled nanotubes were also found among the multi walled nanotubes produced on the carbon/zeolite catalyst. Catalysts such as iron, cobalt and nickel contain either a single metal or a mixture of metals which seem to induce the growth of isolated single walled nanotubes or single walled nanotubes bundles in the ethylene or other atmosphere. The production of single walled nanotubes as well as double walled CNTs on molybdenum and molybdenum-iron alloy catalysts have also been demonstrated. CVD of carbon within the pores of a thin alumina pattern with or without nickel catalyst have been achieved. Ethylene was used with reaction temperature of 550 °C for nickel catalyzed CVD and approximately 900 °C for an un-catalyzed CVD process. The resultant carbon nanostructures have open ends with no caps. Methane has also been continuously used as a carbon source. In particular it has been used to obtain nanotube chips containing isolated single walled nanotubes at different controlled locations. High yields of single walled nanotubes have been obtained by catalytic decomposition of an H<sub>2</sub>/CH<sub>4</sub> mixture over well-dispersed metal particles such as cobalt, nickel and iron on magnesium oxide at approximately 1000 °C. It has been observed that the synthesis of composite powders containing well-dispersed CNTs can be achieved by selective reduction in an H<sub>2</sub>/CH<sub>4</sub> atmosphere of oxide solid solutions between a non-reducible oxide and one or more transition metal oxides. The reduction produces very small transition metal particles at a temperature of approximately

greater than 800 °C. The decomposition of CH<sub>4</sub> over the newly formed nanoparticles prevents their further growth and thus results in a very large quantity of single walled nanotubes and little quantity of multi walled nanotubes.

#### **1.6.4 Ball Milling**

Ball milling and successive annealing is another simple method for the production of CNTs. It is well established that mechanical abrasion can lead to fully nano porous microstructures. It was not clear until few years ago that CNTs of carbon and boron nitride can be produced from these powders by thermal annealing. Basically the method consists of placing graphite powder into a stainless steel container along with four hardened steel balls. The container is cleaned and argon is introduced. The milling is carried out at room temperature for approximately 150 hours. The powder is annealed under an inert gas flow at temperatures of 1400 °C for six hours followed by milling. It is thought that the ball milling process forms nanotube nuclei and the annealing process activates the nanotube growth. Research has shown that this method produces more multi walled nanotubes rather than single walled nanotubes.

#### **1.6.5 Other Methods**

CNTs can also be produced by diffusion flame synthesis, electrolysis, use of solar energy, heat treatment of a polymer, low-temperature solid pyrolysis and other few processes. In flame synthesis, combustion of the hydrocarbon gas provides the temperature required with the remaining fuel easily serving as the required hydrocarbon reagent. Hence, the flame constitutes an efficient source of both energy and hydrocarbon raw material. Combustion synthesis has been shown to be ascendable for large volume production for commercial purpose.



## 1.7 Applications of CNT <sup>[15]</sup>

CNTs have extraordinary electrical conductivity, heat conductivity and mechanical properties. Probably they are the best electron field emitter possible. They are polymers of pure carbon and can be reacted, manipulated using the extremely rich chemistry of carbon. This provides opportunity to modify the structure and to optimize its solubility and dispersion.

Extensively, CNTs are molecularly perfect which means that they are free of property degrading flaws. Their material properties can approach to the very high levels of intrinsic characteristics. These extraordinary characteristics give CNTs potential in numerous applications. They are:

### 1.7.1 Field Emission

CNTs are the best known field emitters of any material. This is because of their high electrical conductivity and unbeatable sharpness of their tip (the sharper the tip, the more concentrated will be an electric field, leading to field emission). The sharper the tip means that they emit at low voltages which acts as an important fact for building electrical devices that utilize this feature. Bucky tubes can carry an amazingly high current density (as high as  $10^{13}$  A/cm<sup>2</sup>). Besides this the current is extremely stable.

Another application of this characteristic is in field-emission flat-panel displays. Instead of a single electron gun (used in CRO), here there is a more electron gun for each pixel in the display. The high current density, low turn on, low operating voltage & steady long-lived behaviour make CNTs attract field emitters to use this application.

Other applications using field-emission characteristics of CNTs include: general cold-cathode lighting sources, lightning arrestors and electron microscope sources.

## **1.7.2 Conductive Plastics**

In the last half century plastics has been used as a replacement for metal. For structural applications, plastics have made tremendous development but simultaneously being good electrical insulators.

This dearth is overcome by loading plastics up with conductive fillers such as carbon black and graphite fibers (used to make golf clubs & tennis rackets). The loading required to provide the necessary conductivity is very high, resulting in heavy parts and for those plastic parts whose structural properties are highly degraded.

It is well known that the higher aspect ratio of filler and the lower loading required in way to achieve a given level of conductivity. CNTs are having highest aspect ratio of any carbon fibers. Additionally, they have natural tendency to form ropes which provides inherently very long conductive pathways even at ultra low loadings.

Applications that make use of above stated behaviour of CNTs include EMI/RFI shielding composites, coatings for enclosures, gaskets, other uses such as electrostatic dissipation (ESD), antistatic materials, even transparent coatings and radar absorbing materials.

## **1.7.3 Energy Storage**

CNTs have the intrinsic characteristics desired in material to be used as electrodes in batteries and capacitors. CNTs have a tremendously high surface area ( $1000 \text{ m}^2/\text{g}$ ), good electrical conductivity and the linear geometry which makes their surface highly accessible to the electrolyte.

Investigation has showed that CNTs have the highest reversible capacity of any carbon material which can be used in lithium-ion batteries as well as CNTs are outstanding materials for super capacitor electrodes and are now being marketed.

CNTs also have various applications in fuel cell components. They have properties like high surface area and thermal conductivity that make them functional as electrode catalyst support in the fuel cells. They may also be used in gas diffusion layers as well as current collectors because of properties like high electrical conductivity. CNTs have high strength and toughness to weight properties that may also prove helpful as part of composite components in fuel cells that can be deployed in transport applications where importance is given to durability.

#### **1.7.4 Conductive Adhesives and Connectors**

The above properties that make CNTs suited as conductive fillers for use in shielding, ESD materials etc make them attractive for electronics materials such as adhesives and other connectors.

#### **1.7.5 Molecular Electronics**

Building of electronic circuits from molecules which acts as essential building blocks of materials is the key component of nanotechnology. In any electronic circuit when the dimensions shrink to the nano scale, the interconnections between switches and other active devices become gradually more vital.

Their geometry, electrical conductivity and ability to be precisely make CNTs best suited for the connections in molecular electronics. They have been established in the form of switches.

#### **1.7.6 Thermal Materials**

The anisotropic thermal conductivity of CNTs is applications where heat needs to move from one place to another like application in electronics, advanced computing where uncooled chips now often reach over 100 °C.

Technologies for creating aligned structures and ribbon of CNTs is a step toward realizing extremely proficient heat conduits. Besides composites with CNTs have been shown dramatically increase the bulk thermal conductivity of small loadings.

### **1.7.7 Structural Composites**

The best properties of CNTs are not limited to electrical and thermal conductivities but also include mechanical properties such as stiffness, toughness, and strength. These properties lead to affluence of applications & exploiting them including advanced composites required for high values of these properties.

### **1.7.8 Fibers and Fabrics**

Fibers spun of pure CNTs have been recently demonstrated and undergoing rapid development along with CNT composite fibers. Such super strong fibers will have applications including body and vehicle arm, transmission line cables, woven fabrics and textiles.

### **1.7.9 Catalyst Supports**

CNTs have an intrinsically high surface area. Every atom is not just on a surface rather each atom is on two surfaces, the inside one and outside. Combined with the ability to attach with any chemical species to their sidewalls provides an opportunity for unique catalytic supports. Their electrical conductivity may also be exploited for new catalysts and catalytic behaviour.

### **1.7.10 Biomedical Applications**

The exploration of CNTs in biomedical applications is just in progress, but has significant potential. Cells have been shown to grow on CNTs & further they appear to have no toxic effect. The cells also do not stay to the CNTs, potentially giving rise to applications such as coatings for prosthetics and anti-fouling coatings for ships.

The ability to chemically modify the sidewalls of CNTs also leads to biomedical applications such as vascular stents, neuron growth, regeneration & many more.

### **1.7.11 Other Applications**

There is a possession of other potential applications for CNTs such as solar collection, nano porous filters, catalyst supports, all sorts of coatings and many more. There are almost certainly many surprising applications for this amazing material that will come to light in the years ahead and which may prove to be the most important and valuable of all.

## Chapter 2

### Literature Review <sup>[16]</sup>

The formation of CNTs is suggested by numerous models through CVD (which are summarized below in Table 2.1). All of these deals with catalytic action and diffusion, nucleation but most do not unite all of the diverse processes which lead to the overall synthesis of CNTs. Much of the literature related to the flame synthesis of CNTs is experimental and observational and do not provide physical insights and characterization of the elementary processes that are vital for developing comprehensive modeling capabilities for describing the CNT formation under different conditions in CVD synthesis. Dissimilar methods have been used. Kuwan and Saito et al. [18] recommended a model that explains nano particle growth from ferrocene in which a two step of catalytic reaction model for the formation of Fe nanoparticles was provided. They incorporated the effect of catalyst deactivation, which should be a necessary component of a comprehensive model. Scott et al. [19] suggested a chemical kinetic model that involves soot nucleation kinetics for simulating the nucleation and growth of carbon nickel clusters and single-walled carbon nanotubes. Dateo et al. [20] presented a chemical model for the fabrication of carbon nanotubes by means of high pressure carbon monoxide (HiPco) as originator. Zhang and Smith et al. [21] advocated a kinetic model for methane decomposition and the development of filamentous carbon on a supported cobalt (Co) catalyst. They measured the effects of catalyst deactivation, metal particle size and the carbon density profiles through the catalyst particle at different reaction times. Perez-Cabero et al. [22] propounded a kinetic study of carbon nanotube production due to the catalytic decomposition of acetylene over an iron-supported catalyst. They scrutinized the effect of reaction conditions on the reaction yield and on the structural and morphological distinctiveness of the carbon products that were obtained. D'Anna et al. [23] projected a

reaction pathway for nanoparticle formation in rich premixed atmospheric ethylene flames with C/O ratios across the soot threshold limit. Endo et al. [24] carried out a CFD study of carbon nanotube construction rates in a CVD reactor supported on the catalytic decomposition of xylene. Hinkov et al. [25] accounted an experimental-modeling study that forecasted the outcome of gas pressure on the growth rates of single walled carbon nanotubes (SWCNTs) formed by the arc-discharge technique. They used the spin and surface CHEMKIN [26] software packages to resolve for the genus transfer and chemical kinetic effects, and included the chemical model for fullerenes developed by Krestinin and Moravsky [27]. Gommaes et al. [28] conducted a combined experimental-kinetic modeling study on the effect of operating conditions on the yield of multi walled CNTs (MWCNTs) in a semi-continuous CVD reactor. They anticipated a simple mathematical model for the reaction rate and used mass spectrometry consequences for the kinetic study, although they did no direct measurement or prediction of the CNT production rates. Their (indirect) kinetic model was based on the rate of ethylene putrefaction rather than actual CNT fabrication. Yu et al. [29] studied the cause of catalyst particle size on the growth rate of CNTs by CVD. They observed that highest growth occurs for an most favorable catalyst particle size, which is 13-15 nm for Fe. They proposed a set of surface reactions and put further a growth rate expression, that qualitatively explains this optimum size, but their study did not presented quantitative numerical results from their model. Table 2.1.1 is provided below for better understanding: Villacampa et al. [30] suggested a rate sculpt for the formation of filamentous carbon due to the catalytic decomposition of methane (to form hydrogen). Although they performed an experimental-numerical study of hydrogen formation, they also included rate equations for the formation of filamentous carbon. Snoeck et al. [31] conducted an analogous experimental-kinetic modeling study of carbon filament formation on Ni particles in which they considered surface reactions, one-dimensional diffusion (based on Fick's law) of carbon through the catalyst particle and a

kinetic prediction of coking threshold. Chen et al. [32] investigated the synthesis of carbon nanofibers by CVD and the effect of Ni crystal size on methane decomposition. A latest exploration by Puretzky et al. [33] proposed a growth rate model for carbon nanotube formation during CVD. They executed in situ measurements and modeled the growth kinetics of vertically aligned nanotube arrays. Their model alerted on CNT growth on a catalyst nanoparticle and suggested some featured scales for CNT extinction times and termination lengths. It is evident from these instances; a variety of models exist for comprehensive or semi-detailed descriptions of the nucleation of carbon nanoparticles and the growth of CNTs.



**Table 2.1** Synthesis of CNTs by Using Different Techniques <sup>[16]</sup>

Authors	Mode of synthesis	Temperature of formation	Source of carbon	Catalyst	Modeling approach
De Chen <i>et al.</i> (2004)	Tapered oscillating element microbalance (TEOM)	580 °C (853 K)	Methane (CH <sub>4</sub> )	Nickel	Modeling of carbon diffusion through Ni metal particles used as catalyst and kinetic effects of Ni crystal size based on a detailed kinetic mechanism of carbon nanofiber growth. The model includes the effect of fast catalyst deactivation and includes thermodynamic effect like the change in the Gibbs free energy and the effect of thermodynamic equilibrium constants.
Scott (2004)	Laser ablation	Temperature drop from 3500 K to 1500 K in ~ 1 μs	Fullerene	Nickel	Chemical modeling of the formation of carbon/nickel clusters.
Zavarukhin and Kuvshinov (2004)	Isothermal perfect-mixing chemical vapor deposition (CVD) reactor	490-590 °C	CH <sub>4</sub> /H <sub>2</sub>	High-loaded nickel catalyst (90 wt. % Ni-Al <sub>2</sub> O <sub>3</sub> )	Mathematical model explaining formation of nanofibrous carbon and process kinetics involving catalyst deactivation.
Kuwana and Saito (2005)	CVD	700 °C (973 K)	Xylene (C <sub>8</sub> H <sub>10</sub> )	Ferrocene [Fe(C <sub>5</sub> H <sub>5</sub> ) <sub>2</sub> ], forming iron nanoparticles	Modeling of formation of Fe nanoparticles in an Eulerian coordinate system. Multi-dimensional computational fluid dynamics (CFD) simulation, including mechanism of nucleation and surface growth on an iron particle after bi-particle collision.
Endo <i>et al.</i> (2004)	CVD	700 °C (973 K)	Xylene (C <sub>8</sub> H <sub>10</sub> )	Iron (Fe) particles	CFD model involving two gas-phase reactions and four surface reactions to predict catalytic formation of CNTs from xylene. Inverse calculations were used, using measurements from exhaust gas.

Authors	Mode of synthesis	Temperature of formation	Source of carbon	Catalyst	Modeling approach
D'Anna <i>et al.</i> (2001)	Flame synthesis, rich premixed flame	1500-1750 K	Ethylene (C <sub>2</sub> H <sub>4</sub> )	None	Reaction pathway for nanoparticle formation.
Zhang and Smith (2005)	CVD	500 °C (773 K)	Methane (CH <sub>4</sub> )	Cobalt (Co)	Model involving the surface catalytic reactions that transfer carbon to solid phase, diffusion of carbon through metal particle, nucleation and growth of carbon nanotubes.
Jourdain <i>et al.</i> (2002)	CVD	1080 °C	Methane (CH <sub>4</sub> )	Ni-Fe	Mechanism of sequential growth, proposed to explain nanotube structure.
Perez-Cabero <i>et al.</i> (2004)	CVD	700 °C	Acetylene (C <sub>2</sub> H <sub>2</sub> )	Fe	Kinetic study including surface catalysis model involving catalysis deactivation.
Puretzky <i>et al.</i> (2005)	CVD	535-900 °C	Acetylene (C <sub>2</sub> H <sub>2</sub> )	Silicon (Si) substrate with evaporated aluminum-iron-molybdenum (Al/Fe/Mo) multi-layered catalyst	Kinetic modeling of CNT formation and growth on a catalyst nanoparticle. Deals with the growth rate of CNT length with addition of carbon nanoparticles to the surface. Both termination time and termination length were modeled and corresponding scales were proposed. Catalyst deactivation (both due to formation of encapsulating carbon as well as due to deposition of acetylene pyrolysis products on the surface) and reactivation were taken accounted for.
Kuwana <i>et al.</i> (2005)	CVD	700 °C (973 K)	Xylene (C <sub>8</sub> H <sub>10</sub> )	Iron (Fe) particles	CFD model involving two gas-phase reactions and four surface reactions to predict catalytic formation of CNTs from xylene. Detailed model for catalyst deactivation was proposed. Inverse calculations were used, using measurements from exhaust gas. Continuation of work by the same group (Endo <i>et al.</i> (2004)).

Authors	Mode of synthesis	Temperature of formation	Source of carbon	Catalyst	Modeling approach
Snoeck <i>et al.</i> (1997)	Methane cracking	773-823 K	Methane (CH <sub>4</sub> )	Nickel (Ni)	Kinetic model study of carbon filament formation on Ni particle, involving surface reaction, one-dimensional diffusion (Fick's law) and kinetic prediction of coking threshold.
Dateo <i>et al.</i> (2002)	High pressure carbon monoxide process	1000-1400 K (appx. 100 atm. pressure)	Carbon monoxide (CO)	Iron pentacarbonyl [Fe(CO) <sub>5</sub> ]	Chemical kinetic models (both detailed and reduced) proposed for surface reactions, iron-carbon cluster formation and carbon nanotube growth.
Villacampa <i>et al.</i> (2003)	Catalytic decomposition of methane	550-800 °C	Methane (CH <sub>4</sub> )	(Nickel-Aluminum oxide) Ni-Al <sub>2</sub> O <sub>3</sub> coprecipitated catalyst	Experimental-numerical work, mainly studying the formation of hydrogen by catalytic decomposition of methane. Growth rate model for formation of filamentous carbon also suggested.
Hinkov <i>et al.</i> (2005)	DC arc-discharge method	Anode temperature 4000-6500 K and cathode temperature 1840 K	Graphite anode	Ni-Yttrium biocatalyst	Experimental-numerical work, studying the effect of gas pressure on SWNT formation
Gommes <i>et al.</i> (2004)	CVD	700 °C (973 K)	Ethylene (C <sub>2</sub> H <sub>4</sub> )	Fe <sub>x</sub> – Co <sub>y</sub> supported on alumina	Experimental-numerical work consisting of a kinetic study of the effect of the operating conditions of a CVD reactor on the yield of multiwalled carbon nanotubes (MWCNTs)
Yu <i>et al.</i> (2005)	CVD	600-650 °C	CO/H <sub>2</sub>	Silica supported Fe	Experimental work with a proposed rate model for the formation of CNTs. The expression of growth rate is used to explain the effect of particle size qualitatively, but there are no quantitative numerical results.
Kamachali (2006)	CVD	600-650 °C (873-1073 K)	C <sub>2</sub> H <sub>2</sub>	Fe	Proposed theoretical model, compared with a few experimental data points from other sources
Larouche <i>et al.</i> (2005)	Plasma torch	1000-1250 K	C particles	Fe/C particles	Solutal Be'nard–Marangoni instability (BMI) theory proposed

**Table 2.2** Synthesis of CNTs by Using Different Carbon Precursors <sup>[17]</sup>

Catalyst precursor compound	Carbon precursor	Additive	Reaction temperature in [ °c]	Support material	Description of synthesized material	References
Fe(NO <sub>3</sub> ) <sub>3</sub>	CH <sub>4</sub>		900	Al <sub>2</sub> O <sub>3</sub> (powder)	SWNT and Bundles, MWNT	[41]
MoO <sub>2</sub> , Fe(NO <sub>3</sub> ) <sub>3</sub>	CO, C <sub>2</sub> H <sub>4</sub>		750-850	Al <sub>2</sub> O <sub>3</sub> (powder)	SWNT and Bundles, MWNT	[42]
Fe(NO <sub>3</sub> ) <sub>3</sub> , Ni(NO <sub>3</sub> ) <sub>2</sub> , Co(NO <sub>3</sub> ) <sub>2</sub>	CH <sub>4</sub>		1000	Al <sub>2</sub> O <sub>3</sub> (powder) and SiO <sub>2</sub> (powder)	SWNT and Bundles	[43]
MoO <sub>2</sub>	CH <sub>4</sub>		850 - 1000	Al <sub>2</sub> O <sub>3</sub> (aerogel)	Bundles of SWNT	[44]
MoO <sub>2</sub>	CO		1200	Al <sub>2</sub> O <sub>3</sub> (powder)	SWNT	[45]
Co(NO <sub>3</sub> ) <sub>2</sub>	CO		700	SiO <sub>2</sub> (gel)	Bundles of SWNT	[46,47]
Cobalt & Iron salts	CH <sub>4</sub>	H <sub>2</sub>	1000	MgO (Powder)	SWNT and Bundles	[48]
Cobalt, Nickel & Iron salts	C <sub>2</sub> H <sub>4</sub>		1080	Al <sub>2</sub> O <sub>3</sub> (Powder), SiO <sub>2</sub> (Powder)	SWNT and Bundles	[49]
Fe(NO <sub>3</sub> ) <sub>3</sub> , Ni(NO <sub>3</sub> ) <sub>2</sub> , Mg(NO <sub>3</sub> ) <sub>2</sub> , Co(NO <sub>3</sub> ) <sub>2</sub>	CH <sub>4</sub>	H <sub>2</sub>	1000-1070	MgO or Mg <sub>0.8</sub> Al <sub>2</sub> O <sub>4</sub> (from combustion)	SWNT and MWNT Individual and Bundles	[50,51]
Fe(NO <sub>3</sub> ) <sub>3</sub>	CH <sub>4</sub>		850	MgO and Si (Wafer)	SWNT and bundles	[52]
Cobalt, Molybdenum	CH <sub>4</sub> , C <sub>2</sub> H <sub>2</sub>		900	SiO <sub>2</sub> (Oxidized Silicon)	Bundles of MWNT	[53,54]
Fe(NO <sub>3</sub> ) <sub>3</sub> , MoO <sub>2</sub>	CH <sub>4</sub>	H <sub>2</sub>	900-1000	Al <sub>2</sub> O <sub>3</sub> (on Si wafer)	SWNT and Bundles	[55,56,57]
Iron	CH <sub>4</sub>		600-800	Sapphire	Bundles of SWNT and MWNT	[58]
Fe <sub>2</sub> O <sub>3</sub> , Iron and Nickel	CH <sub>4</sub>		750-1000	SiO <sub>2</sub> (Oxidized Silicon)	Bundles of MWNT	[59]
Fe(NO <sub>3</sub> ) <sub>3</sub>	C <sub>2</sub> H <sub>2</sub>		600-650	Al <sub>2</sub> O <sub>3</sub> (Powder)	MWNT	[60]
Iron, molybdenum	CO, CH <sub>4</sub>	H <sub>2</sub>	900	Si (Water)	SWNT and Bundles	[61]
Fe(NO <sub>3</sub> ) <sub>3</sub> ,	C <sub>2</sub> H <sub>2</sub>	H <sub>2</sub>	750-1000	Al <sub>2</sub> O <sub>3</sub>	SWNT and	[62]

Ni(NO <sub>3</sub> ) <sub>2</sub> , Co(NO <sub>3</sub> ) <sub>2</sub>				(Powder), SiO <sub>2</sub> (Powder)	MWNT	
Mg(NO <sub>3</sub> ) <sub>2</sub> + (NH <sub>4</sub> ) <sub>6</sub> Mo <sub>7</sub> O <sub>24</sub>	CH <sub>4</sub>	H <sub>2</sub>	1200	MgO (Powder)	MWNT	[63]
Ni(NO <sub>3</sub> ) <sub>2</sub>	C <sub>2</sub> H <sub>2</sub>	H <sub>2</sub>	450-800	Al <sub>2</sub> O <sub>3</sub> (Powder)	MWNT	[64]
Cobalt, Nickel	C <sub>2</sub> H <sub>2</sub>	NH <sub>3</sub>	800-900	SiO <sub>2</sub> (Oxidized silicon)	MWNT	[65]
Nickel, Nickel- Copper	CH <sub>4</sub> , CO	H <sub>2</sub>	450-650	SiO <sub>2</sub> (Oxidized silicon)	MWNT	[66]
Copper, Iron, Nickel	C <sub>2</sub> H <sub>2</sub>	H <sub>2</sub>	750	Al <sub>2</sub> O <sub>3</sub> (Powder) , SiO <sub>2</sub> (Powder), TiO <sub>2</sub> , CaO	MWNT, No tubes on CaO	[67]
Fe(NO <sub>3</sub> ) <sub>3</sub> , Ni(NO <sub>3</sub> ) <sub>2</sub> , Co(NO <sub>3</sub> ) <sub>2</sub>	C <sub>2</sub> H <sub>2</sub>		580-1000	SiO <sub>2</sub> (Powder), Si (wafer)	MWNT	[68]
Fe(NO <sub>3</sub> ) <sub>3</sub> , Ni(NO <sub>3</sub> ) <sub>2</sub> , Co(NO <sub>3</sub> ) <sub>2</sub>	CH <sub>4</sub>	H <sub>2</sub>	< 520	Al <sub>2</sub> O <sub>3</sub> (Powder) ,	MWNT	[69]
Cobalt/Nickel + Pd, Pt or Cr	C <sub>2</sub> H <sub>2</sub>	NH <sub>3</sub> , H <sub>2</sub>	500-550	SiO <sub>2</sub> (Oxidized Silicon)	MWNT, Carbon Onions	[70]

The above shows the compilation of results obtained by CVD using different metal nitrate phases as precursors and different gases, temperatures and support materials.

## Chapter 3

### Experimental Setup and Techniques

#### 3.1 Introduction to Techniques <sup>[1]</sup>

The first experimental proof of carbon nanotubes (CNTs) came in 1991 in the form of multi wall nanotubes (MWNT). The first experimental confirmation of single wall nanotube tubes (SWNT) came in 1993. Since that time, the synthesis methods for CNTs have been developed immensely. Here we deal with the basics of CNT growth and describes several unique CNT growth processes developed for commercial & research purpose.

Production methods for carbon nanotubes (CNTs) can be broadly divided into 2 categories:

- (a) Chemical process
- (b) Physical process

It depends upon the process which is used to extract atomic carbon from the carbon carrying precursors. Chemical methods depends upon the extraction of carbon only through catalytic decomposition of precursors on the transition metal nanoparticles while physical methods also use high energy sources such as plasma or laser ablation to extract the atomic carbon. Usually physical method gives bulk quantities of CNTs which can be treated chemically to remove any carbon soot or nanoparticles present in the mixture. The above two techniques can further be characterized according to the use of other aspects of the synthesis process such as type of precursor and transition metal nanoparticles used. Despite being thoroughly investigated for the last 20 years, CNT growth process has remained controversial up to certain extent. Still the exact dynamics of the growth is ambiguous a general theory has been obtained on a hypothesis which works pretty well. It

is so far been understood that the nanotubes grow from the over saturation of the transition metal nanoparticles with carbon atoms. A diagram is shown below.

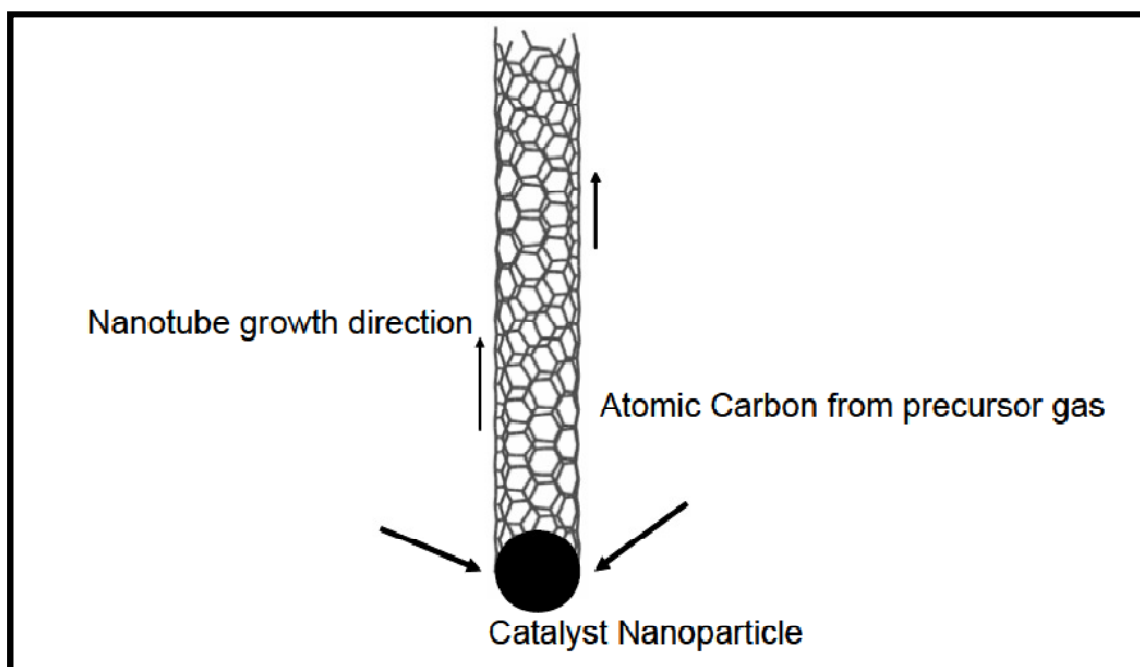


**Figure 3.1** Current CNT growth mechanism hypotheses <sup>[1]</sup>

Transition metal nano particle acts as catalysts which get saturated with atomic carbon to grow nanotubes. The over saturation of nanoparticles with carbon atoms results in the production of different type of molecular carbon species such as graphitic carbon, carbon filaments, multiwall carbon nanotubes, single wall carbon nanotubes and graphene. Selection of the right conditions has remained a trial and error approach to grow these materials (especially nanotube and graphene). This has resulted in excess of CNT growth research papers & most of them are having a explicit guidelines for the growth which makes difficult to replicate in any other system or setup. The controlling of the growth of CNTs has focused more towards chemical vapor deposition (CVD) process where the production of tube is not that high but it can finely be controlled by the use of catalyst nanoparticles.

## 3.2 Chemical Vapour Deposition (CVD) System

Chemical vapor deposition (CVD) is a chemical process used to produce highly purified & highly performance based materials. It is frequently used in the semiconductor industry to produce thin films. In a typical CVD process, the wafer (substrate) is exposed to one or more volatile precursors which react and/or decomposes on the substrate surface to produce the desired result. In lieu volatile by products are also produced which are removed by gas flow through the reaction chamber <sup>[34]</sup>.

Micro fabrication processes generally use CVD to deposit materials in various forms which includes mono-crystalline, polycrystalline, amorphous and epitaxial growth. These materials include silicon, carbon fiber, nanofibers, filaments, carbon nanotubes, SiO<sub>2</sub>, silicon germanium, tungsten, silicon carbide, silicon nitride, silicon oxy-nitride, titanium nitride, and various high k dielectric materials. Synthetic diamonds can also be produced by CVD process.

CVD process consists of placing catalyst nanoparticles (generally on a silicon wafer) in a quartz tube inside furnace which is then heated to the desired growth temperature. Carbon carrier gases are then flown through the quartz tube for a fixed time depending upon the other conditions. After the growth the furnace is cooled down and the wafer is inspected for the resultant nanotube growth. This technique was first used in 2001 to grow single wall carbon nanotubes on flat silicon substrates. The process become popular due to its ability to grow well separated and long single wall carbon nanotubes with less defect density as well as it was having low amorphous carbon content compared to other processes that utilize physical route.

Due to its extensive use in research field, several groups have focused on optimizing the CVD process. Before getting into the details of this technique it will be helpful to look into various parameters that describe this type of growth technique.



### 3.2.1 Types of CVD Process <sup>[34]</sup>

- a) Atmospheric Pressure Chemical Vapour Deposition (APCVD)
- b) Low Pressure Chemical Vapour Deposition (LPCVD)
- c) Metal-Organic Chemical Vapour Deposition (MOCVD)
- d) Plasma Assisted Chemical Vapour Deposition (PACVD) or Plasma Enhanced Chemical Vapour Deposition (PECVD)
- e) Laser Chemical Vapour Deposition (LCVD)
- f) Photochemical Vapour Deposition (PCVD)
- g) Chemical Vapour Infiltration (CVI)
- h) Chemical Beam Epitaxy (CBE)

### 3.2.2 Basic CVD Diagram & Our Lab Setup

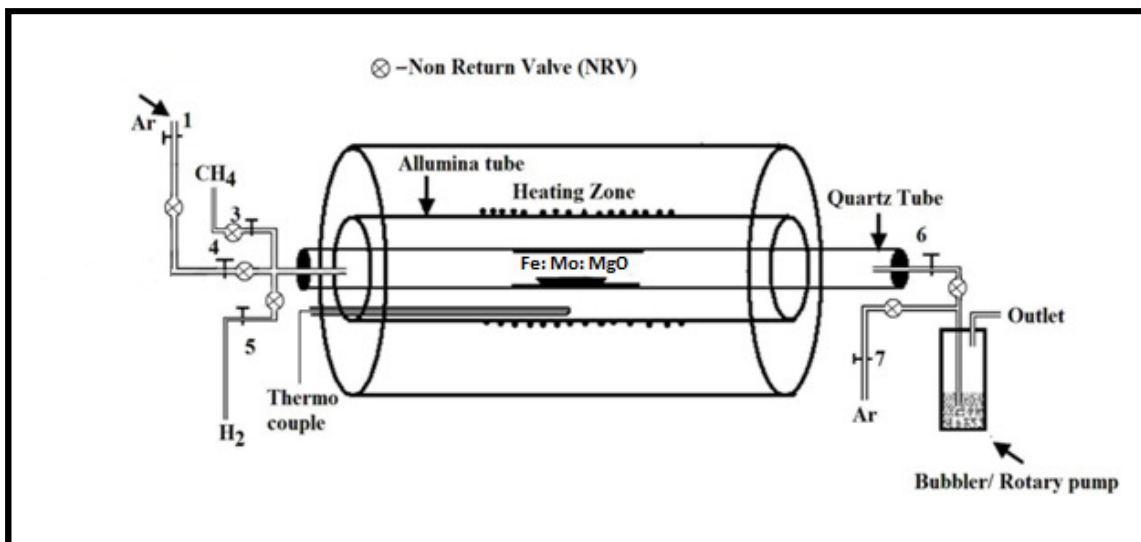


**Figure 3.2** Schematic diagram of chemical vapour deposition (CVD) setup

Inside the quartz tube, a quartz sample holder is used to carry the growth substrate. Flow of gases is controlled through electronic mass flow controllers.

## CVD setup in Nano Fabrication Laboratory at DTU



**Figure 3.3** Microprocessor based controller



**Figure 3.4** Different gas flow controllers and mixtures



**Figure 3.5** Side view of microprocessor controlled furnace



**Figure 3.6** Different cylinders containing 3 gases as argon, methane and hydrogen

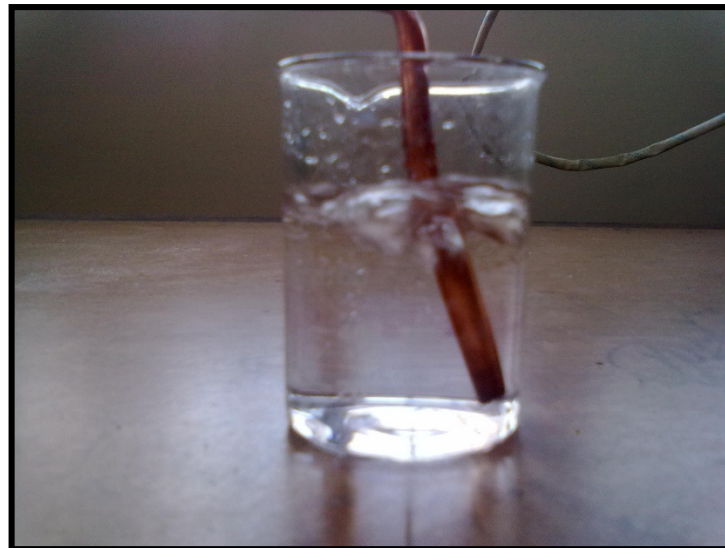


**Figure 3.7** Water filled beaker in which argon is fed through to avoid the oxidation

### 3.2.3 Carbon Precursor

CVD growth of CNTs starts with the gas phase of carbon feedstock. More than a few different carbon containing compounds have been used as precursors such as carbon monoxide (CO), Methane (CH<sub>4</sub>), Ethylene (C<sub>2</sub>H<sub>4</sub>), Acetylene (C<sub>2</sub>H<sub>2</sub>), benzene (C<sub>6</sub>H<sub>6</sub>), toluene (C<sub>7</sub>H<sub>8</sub>), Ethanol (C<sub>2</sub>H<sub>5</sub>OH), and Methanol (CH<sub>3</sub>OH). Each gas has a particular decomposition temperature which results in a different nanotube growth temperature. Let take an example - as CH<sub>4</sub> is known to decompose at very high temperatures (greater than 900 °C) over catalyst nanoparticles whereas C<sub>2</sub>H<sub>5</sub>OH starts self decomposing at temperatures near 800 °C. Although increased temperatures are required for higher rate of nanotube growth and very high temperatures can begin the self dissociation of gases which can cause poison catalyst. The dissociation rates of the precursor can also be controlled by the partial pressure of the species apart from the temperature. Let again take an example - at high pressure CO dissociation rate increases therefore to achieve higher nanotube quantity high pressure CO growth processes are used. A well known example is the HiPco process from Smalley's group at Rice University. Similarly, low pressure growth has also been used to decrease catalyst poisoning to achieve ultra long CNTs. Another important parameter associated with the precursor is its feed rate. At very high temperatures where the precursor is nearly at self dissociation, the reaction rate gets limited by the precursor feed rate in the system. High feed rates can increase the rate of growth but just like high temperatures can also result in more of carbon soot formation and further catalyst poisoning. Precursor feed rate is also coupled with the size of catalytic nanoparticles. At high flow rates larger diameter nanoparticles will grow more since the smaller nanoparticles will quickly get poisoned and vice versa for lower flow rates. In a typical growth situation carbon precursors are premixed with other gases such as H<sub>2</sub> or other carbon carriers (e.g. C<sub>2</sub>H<sub>5</sub>OH + CH<sub>3</sub>OH). This is done to have finer control on the reaction rates inside the CVD chamber. For example if the product after dissociation is H<sub>2</sub> then a fine control of premixed

hydrogen can be used to check on the dissociation rate of carbon precursor. Carbon precursor gases can themselves produce unwanted nanotubes due to the presence of pre mixed nanoparticles occurring from the contamination in the gas cylinder. Gradual changes in growth patterns with change in cylinder pressure due to above conditions. This tells that for a well controlled CVD system, the use of cleaner gases or gas filters is essential in order to achieve reproducible CNT growth.

### **3.2.4 Temperature**

The ideal temperature for CNT growth depends on several factors, mainly carbon feedstock, catalyst and the type of CNTs desired (single, double & multi walled). Nanotubes are typically grown in a temperature range from 500 °C to 1200 °C [35]. Besides to changing the reaction kinetics during growth, the temperature plays an important role in the pre-growth treatment of the catalyst. Small catalytic nanoparticles readily oxidize under ambient conditions. Therefore to bring them back to original state a controlled reduction step is required at moderate temperatures (approximately at 700 °C). Temperature can also significantly affect the growth depending upon ramping rates. Ramping up the furnace temperature at different rates is obtained to have deep effect on the CNT growth kinetics. The role of temperature is becomes more important as nanotube world looks towards the growth of graphene through CVD process.

### **3.2.5 Catalyst Nanoparticle**

Catalysts are transitional metal nanoparticles obtained through various sources such as metal salts, evaporated metal films etc. The two most important factors that define a catalyst particle are its size and composition. Nanoparticles of Fe, Co, Mo, Ni, Cu, Au, etc have been used as catalyst either in pure metallic form or as alloys. These transition metal nanoparticles have common advantages of high carbon solubility, carbon diffusion rates and high melting temperatures. Different approaches are used to obtain the nanoparticles in which some

of them use metal salt (such as nitrates, sulfates and chlorides) where complex stable nanoparticles are formed in the suitable solvent. Evaporated film of metal can also produce uniform nanoparticles upon controlled annealing treatments. For the formation of very small nano size clusters organic carriers have also been used. Sizes of these particles are reported to be anywhere between 1 nm to 15 nm. CNT diameter depends upon the catalyst particles size thus narrowing the catalyst diameter which can help in a controlled diameter nanotube growth. Another important method is to apply the nanoparticles on the growth substrate which affects their resultant morphology significantly <sup>[36]</sup>. Most nanoparticles are suspended in solvents which after drying out on the growth substrate give a coffee stain effects which can be the cause for nanoparticles to bunch before growth making their average size high. Several pioneering methods are used to get rid of this problem. For example, mixing the nanoparticles with polymers before applying on substrates has helped a lot in achieving well separated particles of uniform size. A different promising approach is to mix the particles with PMMA or photo resist and pattern them using lithography techniques. Every approach has its pros and cons and work best for a particular type of CNT growth.

### **3.2.6 Gas Flow Rates**

The flow rate of carbon precursor affects the rate of carbon dissociation during the growth. Gas flow conditions are also responsible in defining CNT length and orientation during their growth. Longer tubes are commonly seen to grow more from wafer edges than the middle of the wafer <sup>[37]</sup>. They are also found to be aligned to the gas flow direction. The observation of wavy tubes is credited to the unsteady flow conditions near the growth wafer (excluding the quartz crystal aligned growth where the mechanism is defective crystal steps). In order to stabilize the near surface flow several techniques have been attempted such as by reducing down the quartz tube cross section and decreasing the flow rates to very low values.

The large variability in nanotube lengths depends upon the type of growth steps. It is accepted that nanotube growth processes are of two kinds:

- (a) Tip growth
- (b) Root growth

In the tip growth process the catalyst nano particle remains in the end of the CNT flowing along with the flow whereas growing CNT in the back. In the root growth process the particle stays on the surface while the tube grows up due to stress induced by carbon atoms saturating the catalyst. Tip based process achieves very long length tubes since metal particle gets saturated in air while flowing.

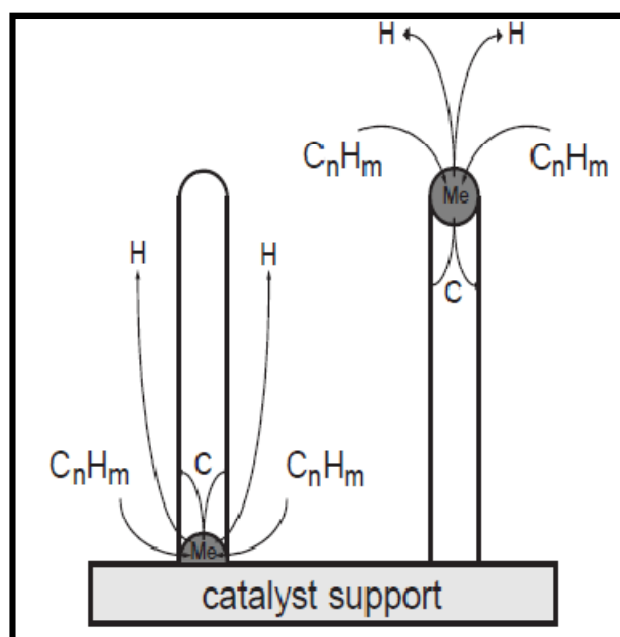


**Figure 3.8** General growth modes of CNT in CVD, Left: Base growth mode & Right: tip growth mode <sup>[38]</sup>

### **3.3 Field Emission Scanning Electron Microscope (FESEM)**

The first practical field emission scanning electron microscope (FESEM) was developed by Hitachi in collaboration with physicist Albert Crewe in 1972 which made possible consistent ultrahigh resolution imaging. The FESEM's initial application was only limited to biology and it captured the first high-resolution images of T<sub>2</sub> bacteriophages (viruses that infect E. coli bacteria). Further detailed images of bacteriophages were produced in the early 1980s with the addition of microprocessor control which made ultrahigh resolution possible at a sub nanometer scale. That also led to the first observation of the AIDS virus in 1985 at Tottori University in Tokyo. A field emission cathode in the electron gun of a scanning electron microscope provides narrower probing beams at both low and high electron energy which results in both improved spatial resolution and minimized sample charging and damage.

#### **Why FESEM?**

- a) FESEM produces lucid and less electro statically distorted images with spatial resolution down to 1.5 nm which is 3 to 6 times better than conventional SEM.
- b) Smaller area contamination spots can be examined at electron accelerating voltages compatible with Energy Dispersive X-ray Spectroscopy.
- c) Reduced penetration of low kinetic energy electrons probes closer to the immediate material surface.
- d) High quality with low voltage images are obtained with negligible electrical charging of samples (accelerating voltages between 0.5 to 30 kV).
- e) Need for conducting coatings to be placed on insulating materials is eliminated.
- f) For ultra high magnification imaging uses our in-lens FESEM.





**Figure 3.9** Basic model of field emission scanning electron microscope (FESEM) <sup>[39]</sup>

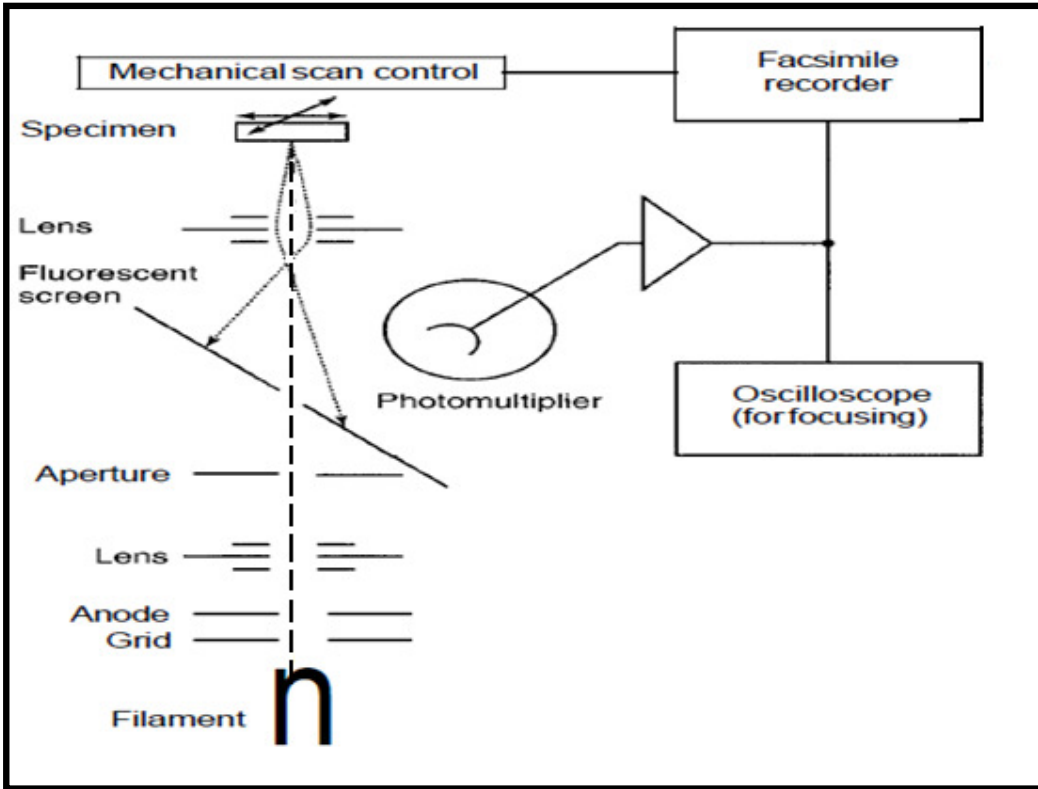


**Figure 3.10** Internal diagram of field emission scanning electron microscope (FESEM) <sup>[39]</sup>

### **3.4 Transverse Electron Microscope (TEM)**

The transmission electron microscope (TEM) operates approximately on the same principle as the light microscope. The TEM has advantage of higher resolution. Due to this we can study detail ultra structure of organelles, viruses and macromolecules. Specifically prepared materials samples may also be viewed in the TEM. It is essential to use the electron beam in a vacuum environment since electrons are very small and easily deflected by hydrocarbons or gas molecules. In order to have an adequate vacuum, series of pumps are used for this purpose. First of all, rotary pumps are used. They are also called the roughing pumps as they are initially used to lower the pressure within the column through which the electron must travel within specified range (10<sup>-3</sup> mm of Hg range). Diffusion Pumps can achieve higher vacuums (10<sup>-5</sup> mm Hg range) but must be backed by the rotary pump. The diffusion pump can also maintain pressure. Additionally turbo, ion or cryo pumps backed by the preceding pumps may be used when an even greater vacuum is required<sup>[40]</sup>.

A nanotube is said to consist of a one-atom thick single-wall nanotube, one tube of graphite or a number of concentric tubes called multi walled nanotubes. When viewed with a transmission electron microscope these tubes appear as planes whereas single walled nanotubes appear as two planes and for multi walled nanotubes more than two planes are observed which can be seen as a series of parallel lines.

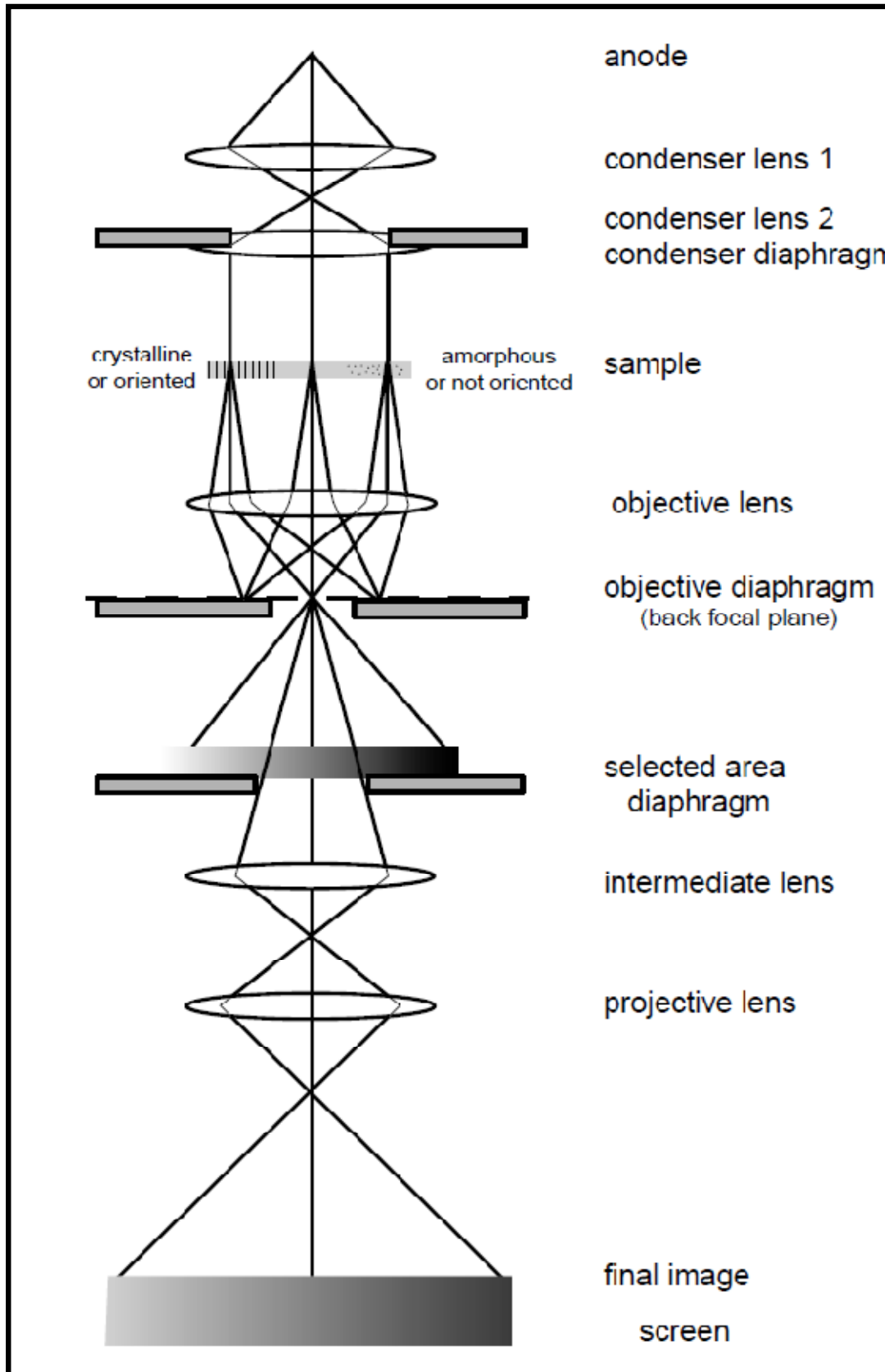
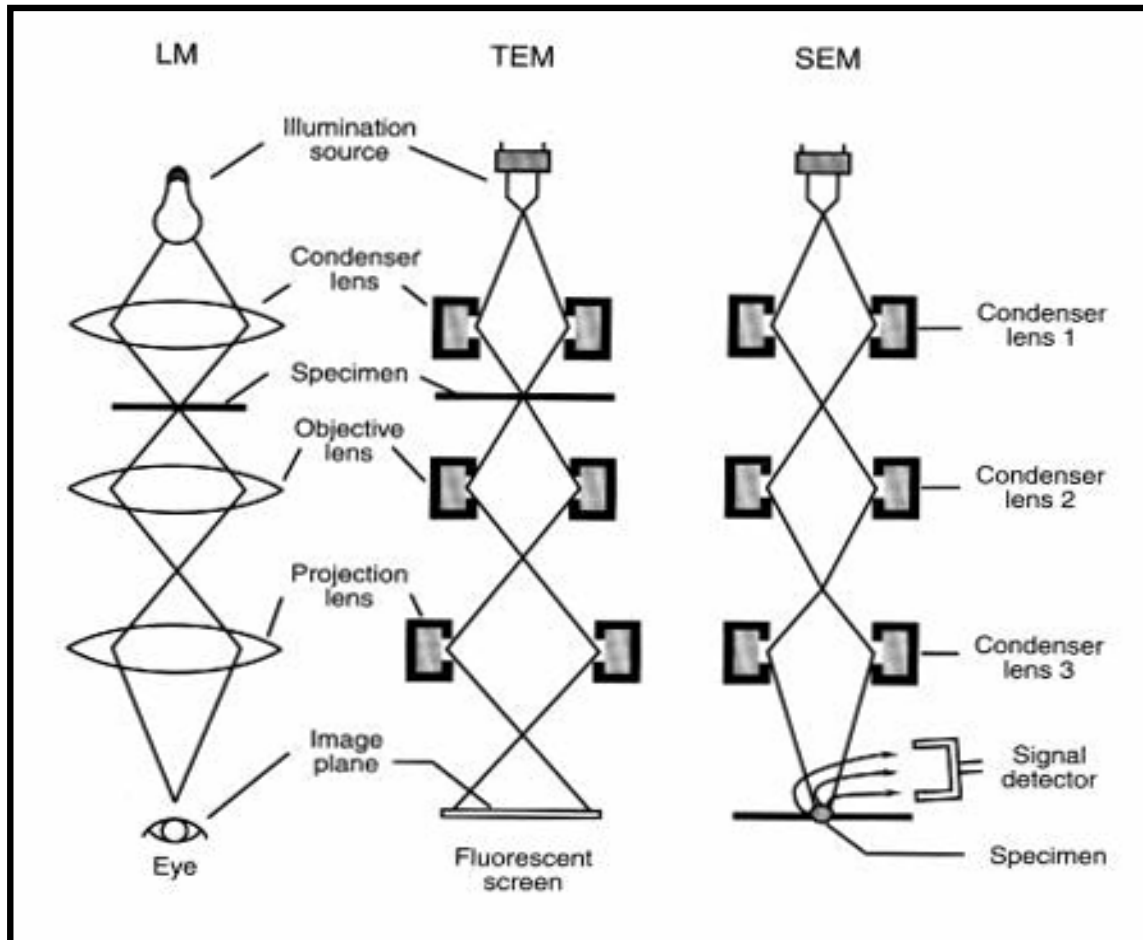


Figure 3.11 Basic internal diagram of transverse electron microscope (TEM) <sup>[40]</sup>



**Figure 3.12** Diagram showing the difference in internal structure of LM, TEM & SEM <sup>[40]</sup>

The illumination source (electron gun) in a thermo ionic emission TEM works similar to a light bulb. A filament (cathode) acts as the source of electrons. It is usually a hairpin shaped tungsten wire. An accelerating voltage (high negative voltage) is applied to the surrounding cathode cap. A small emission current is then applied to the filament in way to release electrons. The point at which the gun achieves good thermal emission as well as an acceptable filament life is called the saturation point. The cathode cap must be slightly more negative than the filament. A resister is located in the gun assembly and is controlled by a knob marked with word bias. It creates the difference in negative voltage between the filament and the cathode cap. This allows the electrons to collect inside the cap forming an electron cloud. An Anode located below the gun assembly is electrically at ground creating a positive

attraction for the negatively charged electrons which further overcomes the negative repulsion of the cathode cap and accelerate through the small hole in the anode.

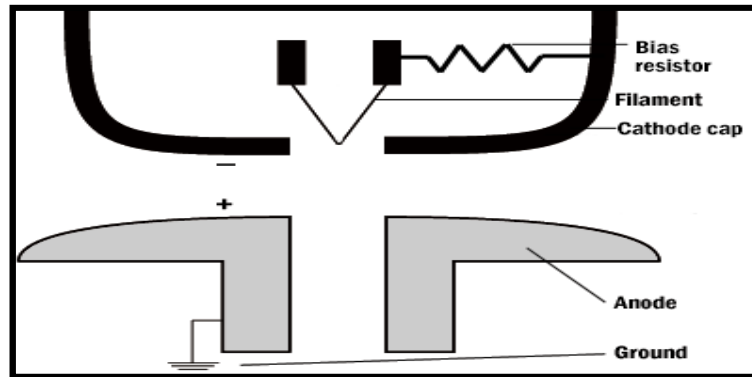


**Figure 3.13** Basic diagram of charge distribution in TEM <sup>[40]</sup>

Glass lenses would obstruct an electron that's why electron microscope (EM) lenses are electromagnetic converging lenses. Copper wire is tightly wound which make up the magnetic field that is the basic nature of the lens. Surrounding these coils is a shroud made of a metal that will not hold magnetic charge when the lens is shut off. The electron moves through the center hole in this solenoid. The electron path is further contracted by a brass lining inside this space known as the pole piece. The pole piece has a small gap within which there is a point where the beam is most influenced by the electromagnetic current. This is suitably referred as the pole piece gap.

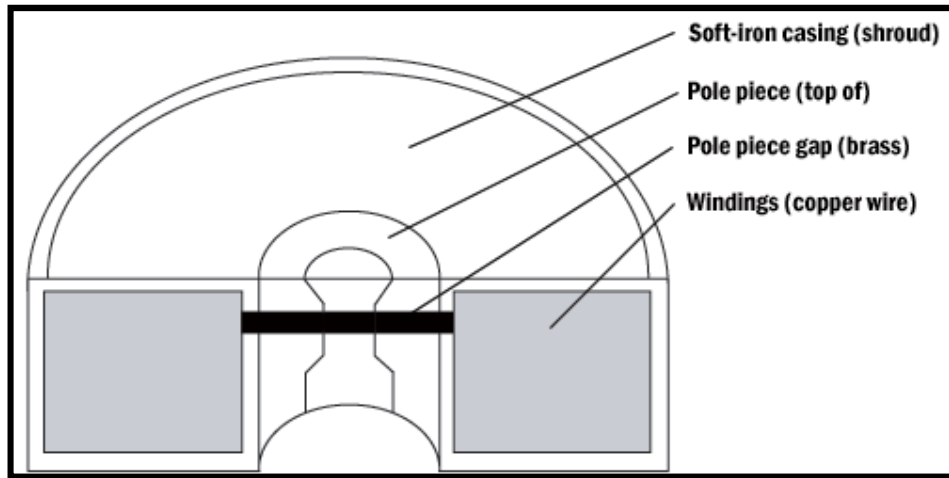


**Figure 3.14** Electromagnetic converging lens of electron microscope <sup>[40]</sup>

Electron paths are generally represented by straight lines running through a convex lens. More precisely the electron paths form a tight spiral as they are accelerated through the lenses. The path and trajectory taken by the electrons are influenced by the lens current when they pass through a small opening in the lens.

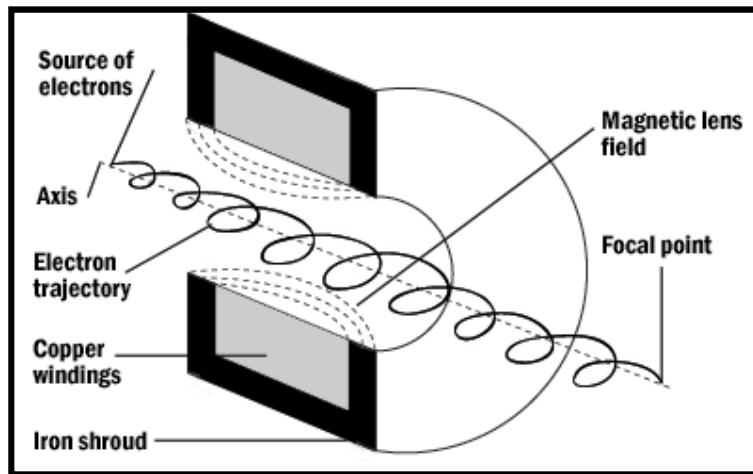


**Figure 3.15** Show actual path of electron in TEM <sup>[40]</sup>

Cross over is the point at which the electrons converge which defines the local length of lens.

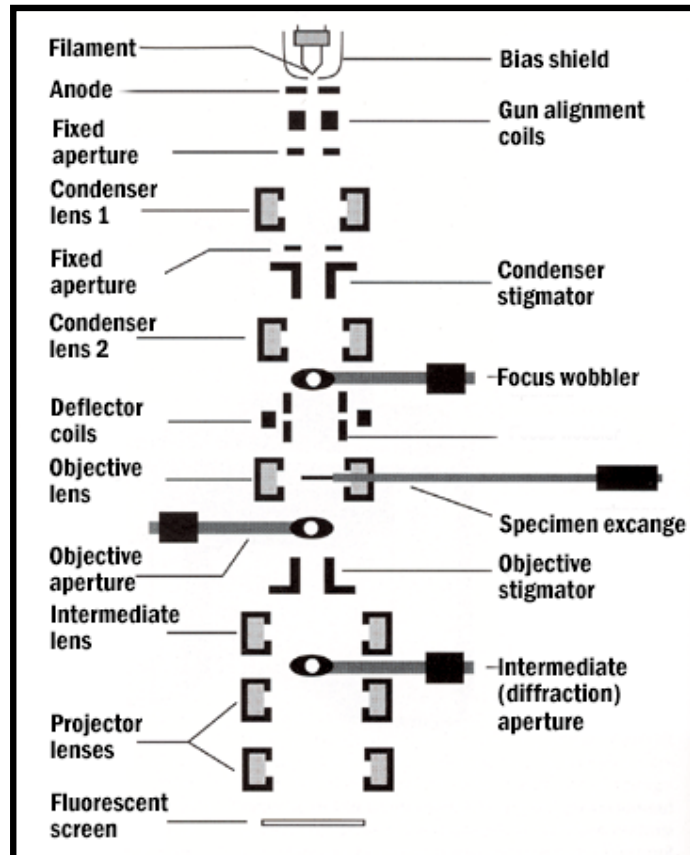


**Figure 3.16** Show different parts of transverse electron microscope (TEM) <sup>[40]</sup>

The condenser lenses in the TEM provide the similar function as that of the condenser in the light microscope. They gather the electrons of the first crossover image and focus them onto the specimen to illuminate the area under examination. A condenser aperture is used in order to reduce spherical aberration. The Objective lens is used mainly to focus and initially magnify the image. The specimen stage is then inserted into the objective lens for imaging purposes. A cold finger or anti contaminator sits near the objective lens. It consists of a thin copper rod at liquid nitrogen temperatures which attracts contaminants. Before the microscope cold finger reservoir must be filled with liquid nitrogen. Contaminants sometimes cause a phenomenon called as drift. Drift is the apparent movement of the specimen across the screen. It is caused by poor contact between the grid and the specimen holder causing a buildup of heat and static charges. Further an objective aperture is used to enhance specimen contrast.

Intermediate lenses magnify the image coming from the objective lens. Finally projector lenses magnify the image coming from the intermediate lens and projects it on the phosphorescent screen.

To optimize the images in the TEM, a beam alignment should be performed prior to its use. There is a special tool for this alignment called as holey grid. A holey grid is a TEM grid support coated with a thin plastic film and stabilizing carbon layer. It is manufactured to contain small round holes helpful in alignment of the TEM. The holes in the grid create Fresnel fringes when the electron beam diffracts around the edges as the electrons come together at over focus. The edge of the hole seems to have bands or fringes.

The final image is viewed onto a phosphorescent screen by projection which gives off photons when irradiated by the electron beam. A camera film is located underneath the phosphorescent screen. The screen is raised to expose a special photographic film with thicker emulsion layer than light film. An alternative option of photographic film is digital capture with a computer digitizing and archiving (CCD) camera.

The operator is responsible for adjustment of variable bias, recognition of aberrations, image drift, photography, specimen contrast, resolution, even illumination and filling the anti contaminators with liquid nitrogen before using the TEM.

Instrument maintenance that requires staff/company repair are filament saturation, filament exchange, aperture cleaning/replacement, specimen holder cleaning, vacuum pump maintenance and screen on which view appears.



## **Chapter 4**

### **Experimental Methodology**

#### **4.1 Accessories Required**

We require so many small items in order to perform the experiment. These apparatus play a vital role in order to obtain the precise result. There are as follows:

Quartz crystalline substrate, Boat, Scissor, Acetone, Tissue paper, 5ml & 10 ml Sample bottles, Plastic zip lock, Cylinder key, Hand gloves etc.

#### **4.2 Experimental Conditions and Procedure**

Here, catalyst is prepared by using sol-gel method. Sigma-Aldrich chemical of purity 5N are used. The chemical used are: iron nitrate ( $\text{Fe}(\text{NO}_3)_3 \cdot 6\text{H}_2\text{O}$ ) and cobalt nitrate ( $\text{Co}(\text{NO}_3)_2 \cdot 6\text{H}_2\text{O}$ ), atomic solution of Mo in water and MgO powder of surface area (BET-42). After evaporating the liquid, dry catalyst powder was calcinated at  $800\text{ }^\circ\text{C}$  for 5 hrs. The schematic diagram illustrations of the experimental conditions are shown below.

Anything shown in the tabular/chart form is very much easier to understand rather than text form. So small chart gives the details about the steps performed during Chemical Vapour Deposition Process (CVD).

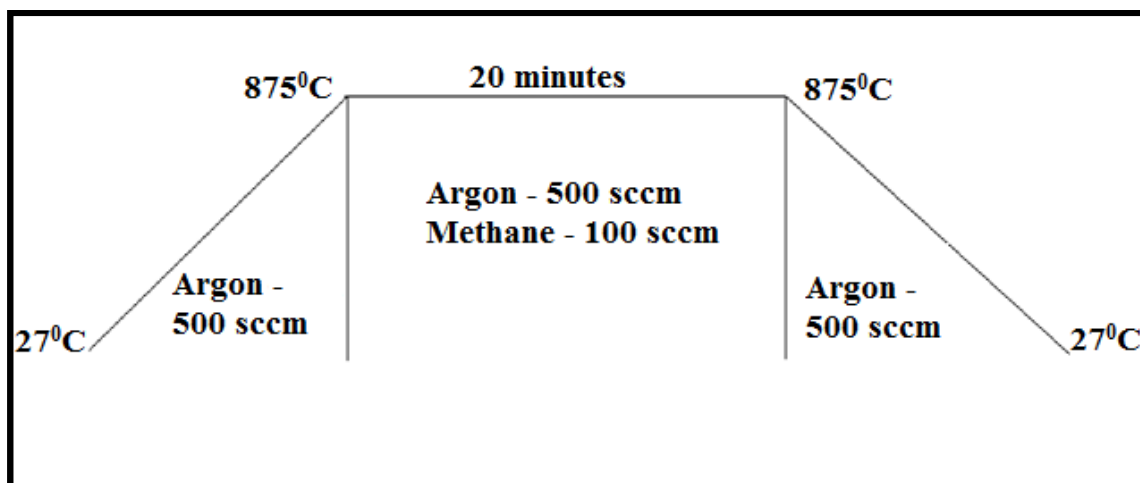


**Figure 4.1** Experimental condition chart

- a) First of all contamination of apparatus was removed by using Acetone (Acid if required).
- b) Then Catalyst Fe:Mo:MgO (7.5:0.75:186.13) and Co:Mo:MgO (1.5:0.75:97.25) in mole ratio was prepared using sol-gel method and then placed uniformly in the boat with proper thickness and further the boat was placed in the centre of the quartz tube.
- c) Further microprocessor based controller was allowed to heat the quartz tube to 875 °C. Simultaneously, Argon gas was passed at 500 sccm till the temperature of 875 °C was obtained.
- d) After reaching the temperature of 875 °C, Methane was passed at 100 sccm for 20 minutes along with Argon.
- e) After 20 minutes, Methane gas was closed and quartz tube was allowed to cool till room temperature 27 °C in presence of Argon gas at 500 sccm in order to prevent oxidation.
- f) Then the Sample in the boat inside the quartz tube was taken out and stored in the glass bottles.
- g) Further the samples were sent to the characterization lab like FESEM, TEM.

## Chapter 5

### Results & Discussion

The various Observation & Results are discussed in this chapter. Although the characterization has been done at different places in order to get the best possible results, altogether they have come to single conclusion which has been discussed here.

#### **5.1 FESEM Images of Carbon Nanotubes**

FESEM images of the as-grown SWNTs using (Fe/Co:Mo:MgO) catalyst are shown in Figure 5.1, 5.2 & 5.3. The low magnification FESEM image reveals that due to unsaturated  $\pi$ -bond SWNTs are grown in entangled carbon filaments which makes cross-linked networks and completely cover the entire catalyst surface as shown in Figure 5.2 (c) & (d). FESEM images also depicts that no amorphous carbon or carbon flakes are attached to SWNTs boundless. As the FESEM images in Figure 5.1, 5.2 & 5.3 shows, in contrast to (Co:Mo:MgO), (Fe:Mo:MgO) offers a very good catalyst for the growth of high density single walled carbon nanotubes. Magnified FESEM image (Fig 5.1) shows that the as-synthesized carbon filaments have uniform diameter ranging from 3 to 15 nm and have smooth surfaces without amorphous carbon particle or disordered graphite, is corroborative evidence of high purity and high yield of as-grown DWCNTs.

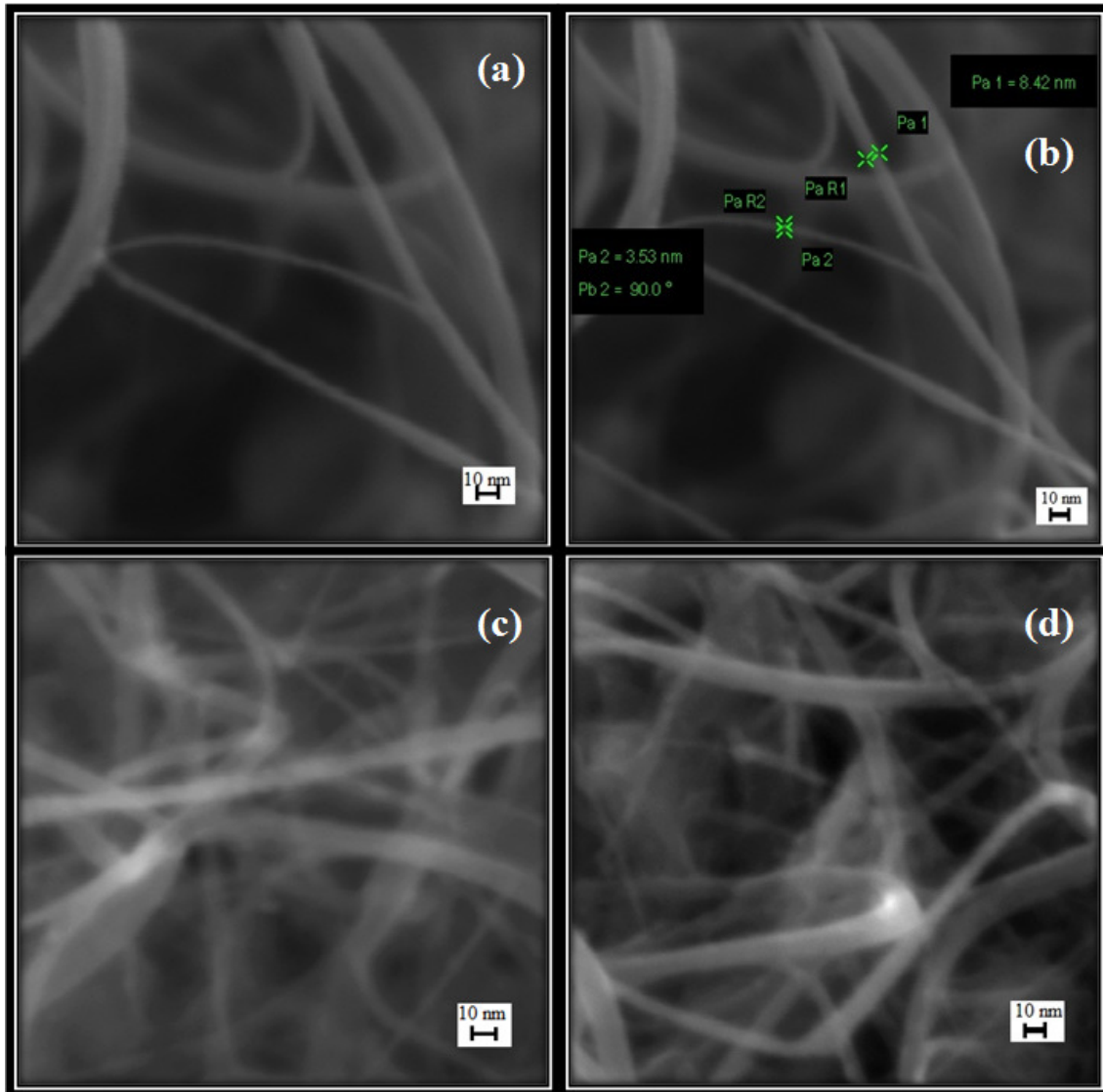


**Figure 5.1** SEM images of the SWCNTs grown in thermal CVD using (Fe:Mo:MgO) catalyst at same magnifications (scale bar is 10 nm)

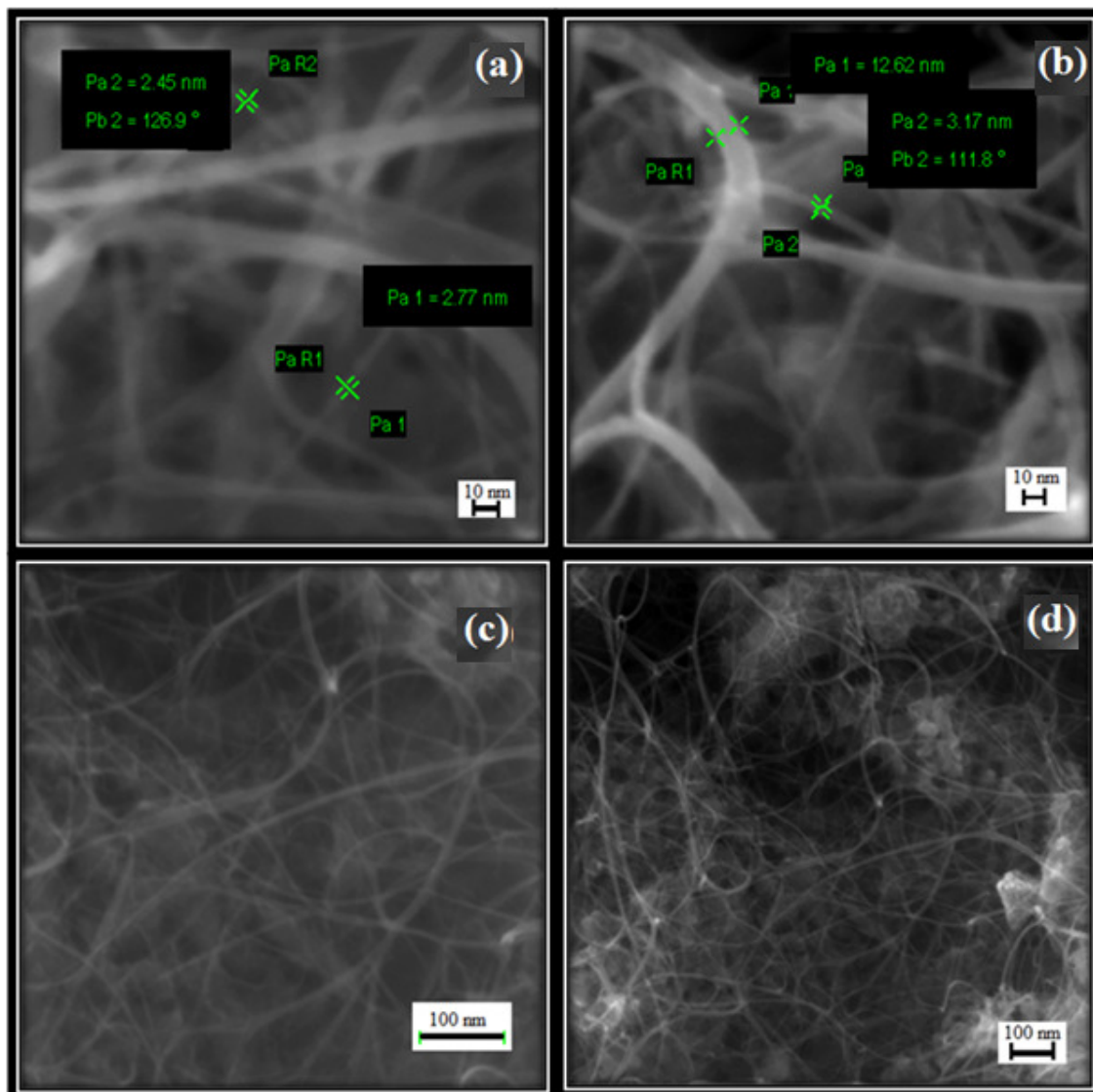


**Figure 5.2** SEM images of the SWCNTs grown in thermal CVD using (Fe:Mo:MgO) catalyst at various magnifications (scale bar of two image is 10 nm & other two is 100 nm)

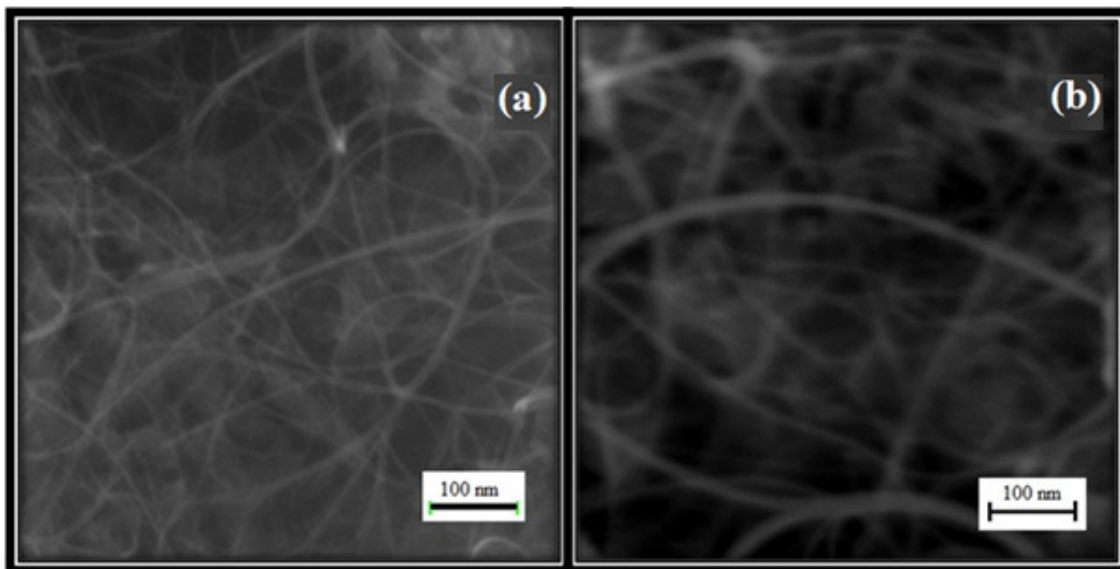


**Figure 5.3** SEM images of the SWCNTs grown in thermal CVD using (Fe:Mo:MgO) catalyst at same magnifications (scale bar is 100 nm)

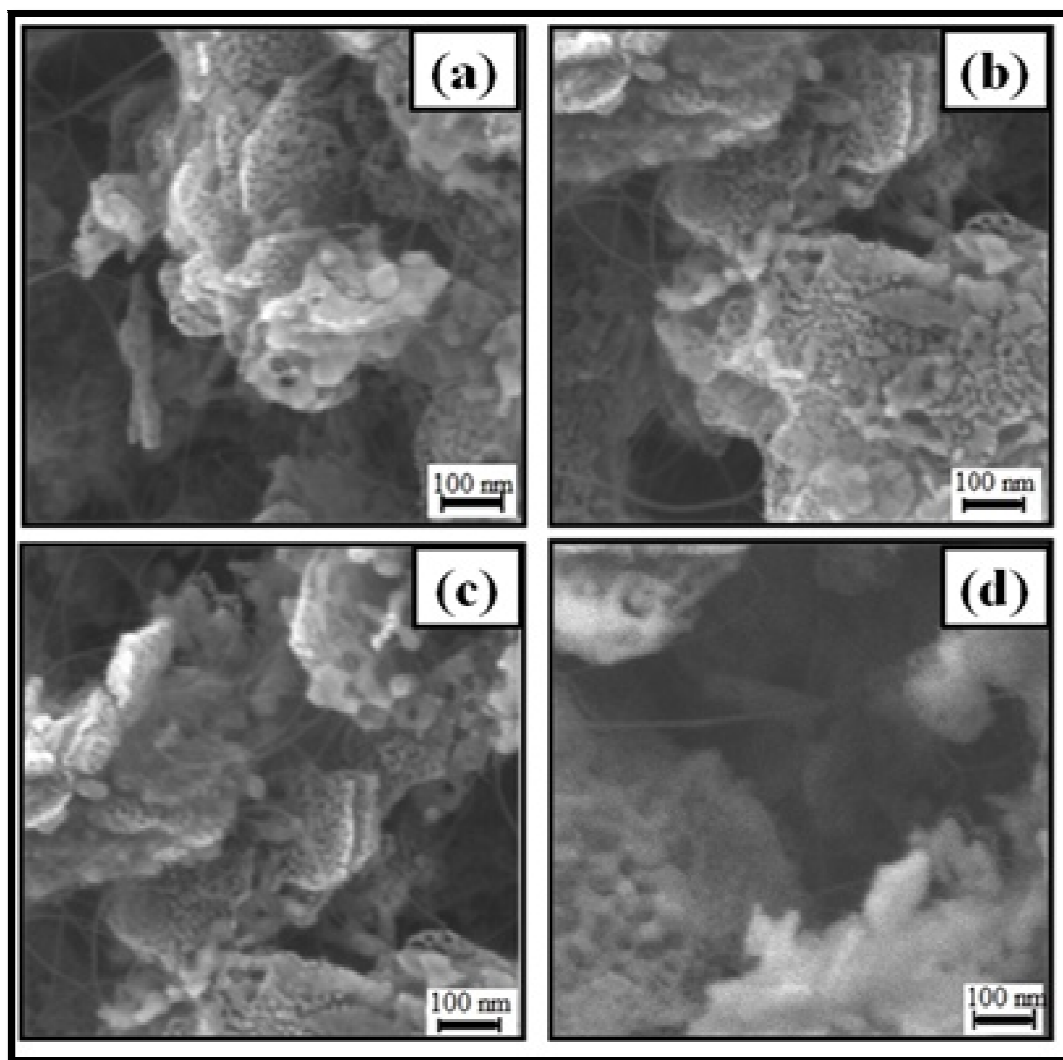


**Figure 5.4:** SEM images of the SWCNTs grown in thermal CVD using (Co:Mo:MgO) catalyst at various magnifications (scale bar is 100 nm) \*

## 5.2 TEM Images of Carbon Nanotubes

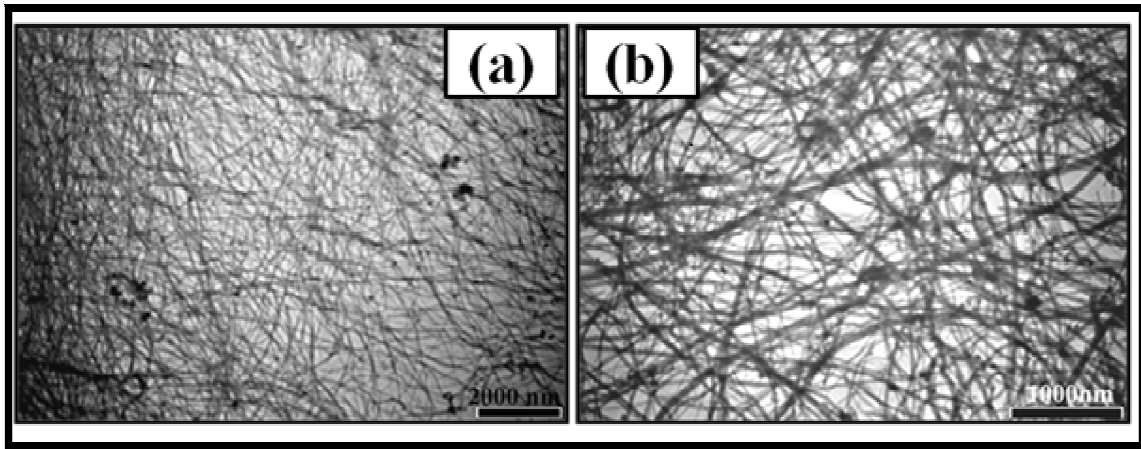


**Figure 5.5** Bright field TEM images of the carbon nanotube grown in thermal CVD using ferrocene used as catalyst (scale bar is 2000 nm & 1000 nm) \*

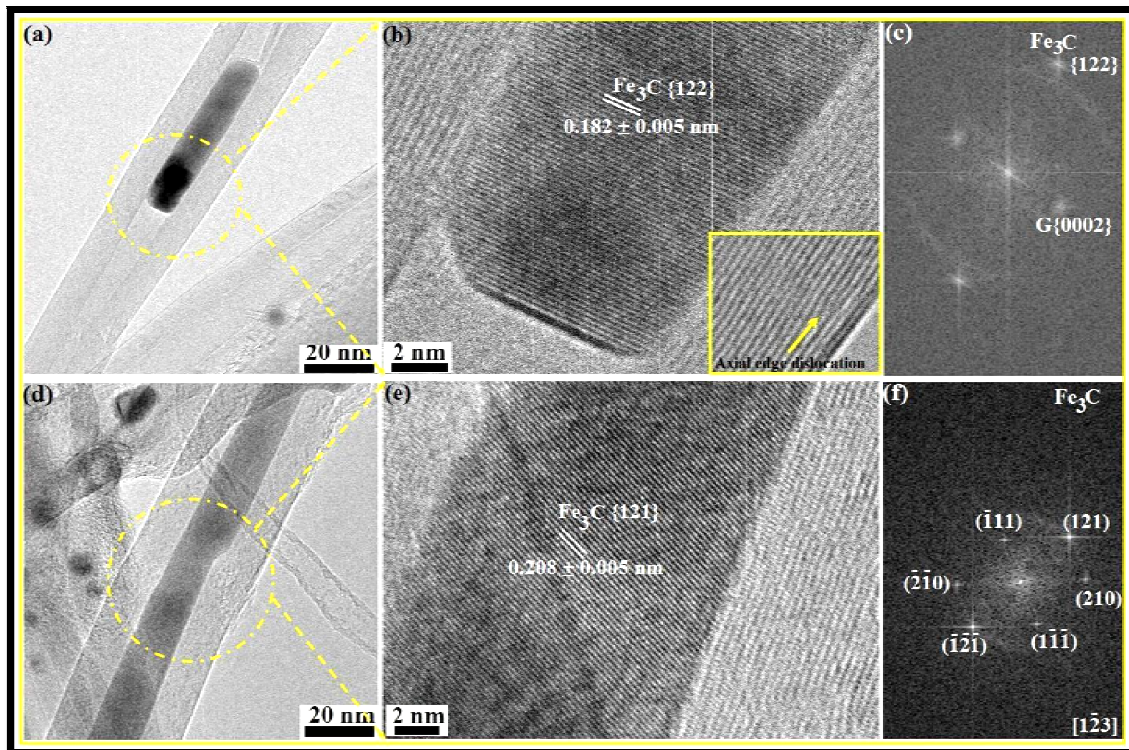


**Figure 5.6** The TEM images of as grown metal-filled MWCNT, Fig (b) & (e) shows the lattice image of nanorod and their corresponding Fourier transforms are also shown in Fig (c)



& (f) respectively. The encapsulated crystal is identified as iron carbide (cementite, Fe<sub>3</sub>C) and viewed along the  $[\bar{1}23]$  direction. In lower set of (b), axial edge dislocation marked by the arrow \*

In Figure 5.6 shows the bright field TEM images obtained at room temperature of an as-grown metal-filled MWCNTs. Lattice projection of CNTs walls in Figures 5.6 (b) & (e) clearly reveals that CNT are multi-walled. The Fig 5.6 (b) reveals that as-grown tubes have high purity. We have not seen any amorphous carbon attached to surfaces of CNTs. Fig 5.6 (a) & (d) reveals that metal nanorod encapsulated inside the CNT. Have diameters of the 10.2 nm and 14.4 nm. Lattice fringes shown in Fig 5.6 (b) & (e) of metal encapsulated within the core of CNT reveal that metal is single crystalline in nature. In the Fig 5.6 (b) lattice fringes with a periodicity of  $0.182 \pm 0.005$  nm, and  $0.208 \pm 0.005$  nm in Fig 5.6 (e) was identified to the {122} planes, and {121} planes of Fe<sub>3</sub>C (orthorhombic structure, space group Pbnm, and the unit cell parameters are  $a=4.523$  Å,  $b=5.089$  Å,  $c=6.7428$  Å). Furthermore, Fourier transform as shown in Fig 5.6 (f) of lattice image reveal that metal crystal is iron carbide (cementite, Fe<sub>3</sub>C) and viewed along the  $[\bar{1}23]$  direction. Since, no diffraction spots splitting observed in the Fourier transform as shown in Fig. 5.6 (c) & (f). Therefore, on the contrary to [10, 11], we assume that encapsulate is pure (i.e. no evidence of coexistence of Fe and Fe<sub>3</sub>C). The failures of producing of pure iron nanorod have been attributed to the strong tendency of forming iron carbide compounds.

A plausible growth mechanism of single walled carbon nanotube is based on various issues. First, owing to a strong interaction between Fe/Co-Mo and MgO support material nanoparticle are neither fluctuating nor migrating on surface MgO support, have stable structure. As the C atoms absorbed on surface of catalyst it formed carbon network (graphene layers) by surface diffusion. Of Course, few carbon atoms diffuse underneath of first atomic layer of catalyst and segregate to active nucleation site and nucleate the in nucleate the second

graphene layer. When kinetic energy is sufficient to overcome the attraction between the graphene and catalyst nano particle then graphene lifts off the catalyst and expels the growth of single walled carbon nanotube. After nucleation of SWCNTs, carbon atoms are incorporated in to SWCNT network at metal-CNT interface.

In addition to above-mentioned observation, our experimental findings demonstrate that iron carbide filled carbon nanotubes directly grow on the bulk quartz substrates. But nanometer sized metal islands on the surfaces are essential pre-request for the nucleation of CNTs. As a first and important issue we have to discuss the different mechanisms for the formation of small metal clusters from which the CNTs grow. In our case, metal islands may form by the dissociation of ferrocene into atomic iron, and then surface diffusion of metal atoms, and eventually Ostwald ripening of metal clusters. After the dissociation, adsorbed atom equilibrates rapidly with the surfaces atoms and diffuse over the surface until it gets trapped at a favourable adsorption site (such as a vacancy or a surface step) and may act as a nucleation centre for the growth of a metal cluster. The activation energy for surface diffusion on Fe on quartz is in the range 0.072 to 0.17 eV. In our case, we have to favour the scenario of clustering of Fe by surface diffusion and then through the Ostwald ripening metal nanoparticles are formed.

As a second issue, we have to understand that at the time of CNT growth whereby the metal clusters are solid or liquid form. There is meanwhile a wide agreement that metal catalyst particles are in the solid state during most CNT growth experiments. Although there is no direct proof, but our results also support this scenario. Faceted tip and the fragmented encapsulation of Fe nanowires in order to accommodate the migrating atoms support the assumption of a solid-state catalyst. It is well-know that liquid should fill the tubes in a more continuous way by capillary forces and formed the tip in a convex, concave and flat shape depending on the surfaces tension.

As the toluene molecules approach the surface, they disassociate in to atomic carbon and then carbon atoms migrate in or on the metal particles. The migration is of further importance, in particular in the context of the question of surface, subsurface, or bulk diffusion. In the case of Fe, the activation energies as obtained by first-principle calculations for surface, sub-surface, and bulk diffusion are 0.57, 0.52 and 0.63 eV, respectively, and thus within a narrow range.

Once nucleated, the CNTs grow on the metal surfaces. The incorporation of carbon in the walls of graphenic layers happens where the layer ends at a surface step on the metal. The high surface diffusion barrier of carbon on Fe may result in aligned graphitic layers. The encapsulation of Fe nanowires may occurs by surface migration of a cluster or individual atoms along the tube axis. Metal atoms may also get trapped in single vacancies and migrate as metal-vacancy complex until an aggregation leads to metal clusters.

## Chapter 6

### Conclusion

As we have seen in the above-mentioned sections, despite extensive progress over the years, there are many basic issues concerning the CNT growth mechanism which are still not clear. Contradictory observations of CNT growth under electron microscopy by different groups suggest that the mechanism is extremely sensitive to each parameter such as carbon precursor, metal catalyst, particle size, temperature, pressure. Even a minor change in any of these parameters leads the growth in critically different directions. Catalysis is the main stem of CVD-CNT technique; and it seems that we have not yet utilized the best of catalysis in this field. New nano-catalyst materials are needed to be developed and investigated in more detail. In principle, with the use of a suitable catalyst, the CVD temperature can be brought down to room temperature. By identifying the growth-limiting steps it should be possible to control the diameter and chirality of the resulting CNTs. To comply with the environmental concerns, renewable materials should be explored as CNT precursors. In view of the expected giant demand of CNTs in the near future, industrial production of CNTs should be carried out with far-sighted thoughts for long-term sustainability. Fossil fuel based CNT-production technology would not be sustainable. The unanswered questions about growth mechanism and the existing problems concerning the growth control will keep the CNT researchers engaged for a long time. Thus, there is no doubt that CNT research will continue to remain a hot topic, a prospective research area.

Finally we have concluded that the sample obtained after CVD process is single walled carbon nanotube with enhanced characteristics. The sample obtained after CVD process was black in colour & in powdered. Only by looking at the sample it is very hard to say whether we have

obtained Carbon nanotube or not. By doing further characterization such as FESEM and TEM of the sample one can be insure about the characteristics of CNTs sample

In this thesis, we have optimized the parameters to grown single walled and metal-filled carbon nanotube. Detailed TEM analysis that  $\text{Fe}_3\text{C}$  encapsulated within the core of MWCNTs is single crystalline in nature, so CNT could be used as template to grow a single crystalline nanowire or rod. To conclude our observation also reveals that the (Fe:Mo:MgO) catalyst are the best catalyst for the growth of single walled carbon nanotubes.

## References

- [1] Bhupesh Chandra – “Synthesis and Electronic Transport in Known Chirality Single Wall Carbon Nanotubes” in Columbia University, 2009.
- [2] History of Carbon and Carbon Materials – “Center for Applied Energy Research at University of Kentucky”. Caer.uky.edu. Retrieved 2008-09-12.
- [3] A G Davies & J M T Thompson – “Advances in Nanoengineering, Electronics Materials & Assembly” Imperial College press Royal Society of Series of Advances Sciences at University of Leeds & University of Cambridge, UK.
- [4] E. Yasude, M. Inagaki, K. Kanako, A. Oya, M. Endo & Y. Tan – “Carbon Alloy, Novel Concepts to Develop Carbon Science & Technology” Elsevier.
- [5] Kroto HW, Heath JR, O’Brian SC, Curl RF, and Smalley RE. C60: Buckminsterfullerene. Nature 1985; 318: 162-163.
- [6] [Physicsworld.com/cws/article/print/1761](http://Physicsworld.com/cws/article/print/1761).
- [7] Smalley RE, Semiconductor cluster surface chemistry. DoD Workshop in Washington, DC (December 1990).
- [8] Dresselhaus MS, Dresselhaus G, and EklundPC. Symmetry for lattice modes in C60 and alkali-metal-doped C60. Phys Rev B 45 1992;12: 6923-6930.
- [9] Krätschmer W, Lamb LD, Fostiropoulos K, and Huffman DR. Solid C60: a new form of carbon. Nature 1990; 347: 354-356.
- [10] Iijima S. Helical microtubules of graphitic carbon. Nature 1991; 354: 56-58.
- [11] Iijima S and Ichihashi T. Single-shell carbon nanotubes of 1 nm diameter. Nature 1993; 363: 603.
- [12] Bethune DS, Kiang CH, de Vries MS, Gorman G, Savoy R, Vasquez J, and Beyers R.

- Cobaltcatalysed growth of carbon nanotubes with single-atomic-layer walls. *Nature* 1993; 363:605.
- [13] Sinnott, S.B.; Andrews, R. (2001). "Carbon Nanotubes: Synthesis, Properties, and Applications". *Critical Reviews in Solid State and Materials Sciences* 26 (3): 145–249.
- [14] *Nanotechnology: Basic Science and Emerging Technologies*”, M. Wilson et al, Chapman and Hall (2002).
- [15] Article ID No.980 on azonano as main source from Carbon Nanotechnologies, Inc.
- [16] Sayangdev Naha – “Growth Model, Synthesis of Carbon Nanostructures and Alteration of Surface Properties Using them” PhD Dissertation Submitted to the Faculty of Virginia Polytechnic Institute & State University on 07/25/2008 Blacksburg, Virginia.
- [17] Kuno Matzinger -“Evolution of Metal Catalyst During CVD Synthesis of Carbon Nanotubes” Dissertation Nr. 1504 ABC Druck & Kopie GmbH, Luzern 2006.
- [18] Kuwana, K., and Saito, K., Modeling CVD synthesis of carbon nanotubes: Nanoparticle formation from ferrocene. *Carbon* 43(10):2088-95 (2005).
- [19] Scott, C.D., Chemical Models for Simulating Single-Walled Nanotube Production in Arc Vaporization and Laser Ablation Processes. *Journal of Nanoscience and Nanotechnology* 4(4):368-76 (2004).
- [20] Dateo, C.E., Gokcen, T., and Meyyappan, M., Modeling of the HiPco Processes for Carbon Nanotube Production. I. Chemical Kinetics. *Journal of Nanoscience and Nanotechnology* 2(5):523-34 (2002).
- [21] Zhang, Y., and Smith, K.J., A kinetic model of CH<sub>4</sub> decomposition and filamentous carbon formation on supported Co catalysts. *Journal of Catalysis* 231(2):354-64 (2005).

- [22] Perez-Cabero, M., Romeo, E., Royo, C., Monzon, A., Guerrero-Ruiz, A., and Rodriguez-Ramos, I., Growing mechanism of CNTs: a kinetic approach. *Journal of Catalysis* 224(1):197-205 (2004).
- [23] D'Anna, A., Violi, A., D'Alessio, A., and Sarofim, A.F., A reaction pathway for nanoparticle formation in rich premixed flames. *Combustion and Flame* 127(1-2):1995-2003 (2001).
- [24] Endo, H., Kunawa, K., Saito, K., Qian, D., Andrews, R., and Grulke, E.A., CFD prediction of carbon nanotube production rate in a CVD reactor. *Chemical Physics Letters* 387(4-6):307-11 (2004).
- [25] Hinkov, I., Farhat, S., and Scott, C.D., Influence of the gas pressure on single-wall carbon nanotube formation. *Carbon* 43(12):2453-62 (2005).
- [26] Kee, R.J., Rupley, F.M., and Miller, J. A., CHEMKIN: A Fortran chemical kinetics package for the analysis of gas phase chemical kinetics. Sandia National Laboratories Report No. 89-8009B.
- [27] Krestinin, A.V., and Moravsky, A.P., Mechanism of fullerene synthesis in the arc reactor. *Chemical Physics Letters* 286(5):479-84 (1998).
- [28] Gommes, C., Blacher, S., Bossuot, Ch., Marchot, P., Nagy, J.B., and Pirard, J.-P., Influence of the operating conditions on the production rate of multi-walled carbon nanotubes in a CVD reactor. *Carbon* 42(8-9):1473-82 (2004).
- [29] Yu, Z., Chen, D., Totdal, B., and Holmen, A., Effect of catalyst preparation on the carbon nanotube growth rate. *Catalysis Today* 100(3-4):261-7 (2005).



- [30] Villacampa, J.I., Royo, C., Romeo, E., Montoya, J.A., Del Angel, P., and Monzon, A., Catalytic decomposition of methane over Ni-Al<sub>2</sub>O<sub>3</sub> coprecipitated catalysts: Reaction and regeneration studies. *Applied Catalysis A* 252(2):363-83 (2003).
- [31] Snoeck, J.-W., Froment, G.F., and Fowles, M., Kinetic Study of the Carbon Filament Formation by Methane Cracking on a Nickel Catalyst. *Journal of Catalysis* 169(1):250-62 (1997).
- [32] S. Iijima, T. Ichihashi: Single-shell carbon nanotubes of 1-nm diameter, *Nature* 363 (1993) 603–605.
- [33] Puretzky, A.A., Geohegan, D.B, Jesse, S., Ivanov, I.N., and Eres, G., In situ measurements and modeling of carbon nanotube array growth kinetics during chemical vapor deposition. *Applied Physics A* 81:223-40 (2005).
- [34] H. O. Pierson, *Handbook of Chemical Vapor Deposition*, Noyes Publications, Park Ridge (1992)
- [35] Harris PJF, *Carbon nanotubes and related structures – New materials for the twenty first century*. Cambridge University Press, Cambridge, UK, 1999.
- [36] Nanotube Modeler, JCrystalSoft 2004 – 2005, <http://www.icrystal.com>.
- [37] Dai H, Rinzler AG, Nikolaev P, Thess A, Colbert DT, Smalley RE. Single-wall nanotubes produced by metal-catalyzed disproportionation of carbon monoxide. *Chem. Phys. Lett.* 1996; 260: 471-475.
- [38] Dresselhaus MS, Dresselhaus G, Avouris Ph (Eds.). *Carbon Nanotubes*. Springer-Verlag, Berlin, Heidelberg 2001
- [39] The Institute of IEEE.org – “Field Emission Scanning Electron Microscope Earns Milestone”

- [40] Article by Central Microscopy Research Facility, part of University of Iowa Vice President for Research, CMRF, The University of Iowa, Iowa
- [41] Cassell A, Raymakers J, Kong J, Dai H, Large scale CVD synthesis of single-walled carbon nanotubes. *J. Phys. Chem.* 1999; 103: 6484-6492.
- [42] Hafner JH, Bronikowski MJ, Azamian BR, Nikolaev P, Rinzler AG, Colbert DT, Smith KA, Smalley RE. Catalytic growth of singlewall carbon nanotubes from met particles. *Chem. Phys. Lett.* 1998; 296: 195-202.
- [43] Kong J, Cassell AM, Dai H. Chemical vapour deposition of methane for single-walled carbon nanotubes. *Chem. Phys. Lett.* 1998; 292: 567-574
- [44] Su M, Zheng B, Liu J. A scalable CVD method for the synthesis of single-walled nanotubes with high catalyst productivity. *Chem. Phys. Lett.* 2000; 322: 321-32
- [45] Dai H, Rinzler AG, Nikolaev P, Thess A, Colbert DT, Smalley RE. Single-walled nanotubes produced by metal-catalyzed disproportionation of carbon monoxide. *Chem. Phys. Lett.* 1996; 260: 471-475.
- [46] Alvarez WE, Kitiyanan B, Borgna A, Resasco DE. Synergism of Co and Mo in the catalytic production of single-wall carbon nanotubes by decomposition of CO. *Carbon* 2001; 39:547-558
- [47] Kitiyanan B, Alvarez WE, Harwell JH, Resasco DE. Controlled production of single-wall carbon nanotubes by catalytic decomposition of CO on bimetallic Co-Mo catalysts. *Chem. Phys. Lett.* 2000; 317: 497-503
- [48] Colomer JF, Stephan C, Lefrant S, Van Tendeloo G, Willems I, Konya Z, Fonseca A. Laurent C, Nagy JB. Large-scale synthesis of single-wall carbon nanotubes by catalytic chemical vapor deposition (CCVD) method. *Chem. Phys. Lett.* 2000; 317: 83-89
- [49] Colomer JF, Bister G, Willems I, Konya Z, Fonseca A. Laurent C, Nagy JB. Synthesis

- of single-wall carbon nanotubes by catalytic decomposition of hydrocarbons. *Chem. Commun.* 1999; 1343-1344
- [50] Flahaut E, Govindaraj A, Peigney A, Laurent C, Rousset A, Rao CNR. Synthesis of singlewalled carbon nanotubes using binary (Fe,Co, Ni) alloy nanoparticles prepared in situ by the reduction of oxide solid solutions. *Chem. Phys. Lett.* 1999; 300: 236-242
- [51] Flahaut E, Peigney A, Laurent C, Rousset A. Synthesis of single-walled carbon nanotube-Co-MgO composite powders and extraction of the nanotubes. *J. Mater. Chem.* 2000; 10:249-252
- [52] Yan H, Li Q, Zhang J, Liu Z. Possible tactics to improve the growth of single-walled carbon nanotubes by chemical vapor deposition. *Carbon* 2002; 40: 2693-2698
- [53] Yoon YJ, Bae JC, Baik HK, Cho SJ, Lee SJ, Song KM, Myung NS. Nucleation and growth control of carbon nanotubes in CVD process. *Physica B Condensed Matter.* 2002;323: 318-320
- [54] Yoon YJ, Bae JC, Baik HK, Cho SJ, Lee SJ, Song KM, Myung NS. Growth control of single and multi-walled carbon nanotubes by thin film catalyst. *Chem. Phys. Lett.* 2002;366: 109-114
- [55] Kong J, Soh HT, Cassell AM, Quate CF, Dai H. Synthesis of individual single-walled carbon nanotubes on patterned silicon wafers. *Nature* 1998; 395: 878-818
- [56] Franklin NR, Li Y, Chen RJ, Javey A, Dai H. Patterned growth of single-walled carbon nanotubes on full 4-inch wafers. *Appl. Phys. Lett.* 2001; 79: 4571-4573
- [57] Soh HT, Quate CF, Morpurgo AF, Marcus CM, Kong J, Dai H, Integrated nanotube circuits: Controlled growth and ohmic contacting of single-walled carbon nanotubes. *Appl. Phys. Lett.* 1999; 75: 627-629
- [58] Hongo H, Yudasaka M, Ichihashi T, Nihey F, Iijima S. Chemical vapor deposition of single-wall carbon nanotubes on iron-filmcoated sapphire substrates. *Chem. Phys. Lett.*

- 2002; 361: 349-354
- [59] Homma Y, Yamashita T, Finnie P, Tomita M, Ogino T. Japan. J. Appl. Phys. 2002; 41: L89-91
- [60] Emmenegger C, Bonard JM, Mauron Ph, Sudan P, Lepora A, Grobety B, Züttel A, Schlapbach L. Synthesis of carbon nanotubes over Fe catalyst on aluminum and suggested growth mechanism. Carbon 2003; 41: 539-547
- [61] Huang S, Woodson M, Smalley RE, Liu J. Growth mechanism of oriented long singlewalled carbon nanotubes using “Fast-Heating”chemical vapour deposition process. Nano Lett 2004; 4 (6): 1025-1028
- [62] Ivanov V, Fonseca A, Nagy JB, Lucas A, Bernaerts A, Zhang XB, Catalytic production and purification of nanotubules having fullerene-scale diameters. Carbon 1995; 33 (12): 1727-1738.
- [63] Pérez-Mendoza M, Vallés C, Maser WK, Martínez MT, Benito AM. Influence of molybdenum on the chemical vapour deposition production of carbon nanotubes. Nanotechnology 2005; 16: 224-225
- [64] Zheng GB, Kouda K, Sano H, Uchiyama Y, Shi YF, Quan HJ. A model for the structure and growth of carbon nanofibres synthesized by the CVD method using nickel as a catalyst. Carbon 2004; 42: 635-640
- [65] Lee CJ, DW Kim, Lee TJ, Choi YC, Park YS, Lee YH, Kim JM. Synthesis of aligned carbon nanotubes using thermal chemical vapour deposition. Chem. Phys. Lett. 1999; 312: 461-468.
- [66] Alstrup I, Tavares, MT Bernardo CA, Sorensen O, Rostrup-Nielson JR. Carbon formation on nickel and nickel-copper alloy catalysts. Mater. Corr. 1998; 49: 367-372
- [67] Vander Wal RL, Ticich TM, Curtis VE. Substrate-support interactions in metalcatalyzed carbon nanofiber growth. Carbon 2001; 39: 2277-2289.

- [68] Klinke C, Bonard JM, Kern K. Comparative study of the catalytic growth of patterned carbon nanotube films. *Surf. Sci.* 2001; 492:195-201.
- [69] Wang X, Hu Z, Chen X, Chen Y. Preparation of carbon nanotubes and nano-particles by microwave plasma-enhanced chemical vapour deposition. *Scripta Mater.* 2001; 44: 1567-1570.
- [70] Lee CJ, Park J, Kim JM, Huh Y, Lee JY, No KS. Low-temperature growth of carbon nanotubes by thermal chemical vapour deposition using Pd, Cr, and Pt as co-catalyst. *Chem. Phys. Lett.* 2000; 327: 277-283.